RL-TR-94-172
Final Technical Report
September 1994

EFFECT OF CELL SIZE ON ELLIPTICALLY POLARIZED RADAR CLUTTER STATISTICS

University of Texas at Arlington

Adrian K. Fung

APPROVED FOR PUBLIC RELEASE; DISTRIBUTION UNLIMITED.

Rome Laboratory
Air Force Materiel Command
Griffiss Air Force Base, New York

This report has been reviewed by the Rome Laboratory Public Affairs Office (PA) and is releasable to the National Technical Information Service (NTIS). At NTIS it will be releasable to the general public, including foreign nations.

RL-TR-94-172 has been reviewed and is approved for publication.

APPROVED: Lisa M Mockapetris

LISA M. MOCKAPETRIS
Project Engineer

FOR THE COMMANDER: Robert V. McGahan

ROBERT V. McGAHAN
Acting Director
Electromagnetics & Reliability Directorate

If your address has changed or if you wish to be removed from the Rome Laboratory mailing list, or if the addressee is no longer employed by your organization, please notify RL (ERCE) Hanscom AFB MA 01731. This will assist us in maintaining a current mailing list.

Do not return copies of this report unless contractual obligations or notices on a specific document require that it be returned.

REPORT DOCUMENTATION PAGE

Form Approved
OMB No. 0704-0188

1. AGENCY USE ONLY (Leave Blank)	2. REPORT DATE	3. REPORT TYPE AND DATES COVERED
	September 1994	Final ----

4. TITLE AND SUBTITLE

EFFECT OF CELL SIZE ON ELLIPTICALLY POLARIZED RADAR CLUTTER STATISTICS

5. FUNDING NUMBERS

C - F19628-91-K-0013
PE - 61102F
PR - 2305
TA - J4
WU - 67

6. AUTHOR(S)

Adrian K. Fung

7. PERFORMING ORGANIZATION NAME(S) AND ADDRESS(ES)

E.E. Department, Box 19016
University of Texas at Arlington
Arlington TX 76019

8. PERFORMING ORGANIZATION REPORT NUMBER

N/A

9. SPONSORING/MONITORING AGENCY NAME(S) AND ADDRESS(ES)

Rome Laboratory (ERCE)
31 Grenier Street
Hanscom AFB MA 01731-3010

10. SPONSORING/MONITORING AGENCY REPORT NUMBER

RL-TR-94-172

11. SUPPLEMENTARY NOTES

Rome Laboratory Project Engineer: Lisa M. Mockapetris/ERCE/(617) 377-9196

12a. DISTRIBUTION/AVAILABILITY STATEMENT

Approved for public release; distribution unlimited.

12b. DISTRIBUTION CODE

13. ABSTRACT (Maximum 200 words)

In this final report, we summarize the approach used and relevant information for simulation of radar signal statistics from randomly rough surfaces. The total number of cases to be performed in this contract is 60 and is depicted in Table 1. Two sets of cases reported in the past are: (1) 30 cases for receiver orientation angles of 135 degrees, five azimuthal angles, three cell sizes with signal distributions expressed in both field amplitude and power; and (2) 12 cases for receiver orientation angle of 45 degrees at azimuthal angles of 180 and 135 degrees, three cell sizes with signal distributions expressed in both field amplitude and power. Additional calculations to be given in this report are for receiver orientation angle of 45 degrees at azimuthal angles of 90°, 45°, and 0° corresponding to 18 cases. For the sake of completeness, all results reported earlier are included in Appendix B.

14. SUBJECT TERMS

Scattering statistics, Rough surface scattering, Elliptical polarization, Kirchhoff current density

15. NUMBER OF PAGES

88

16. PRICE CODE

17. SECURITY CLASSIFICATION OF REPORT	18. SECURITY CLASSIFICATION OF THIS PAGE	19. SECURITY CLASSIFICATION OF ABSTRACT	20. LIMITATION OF ABSTRACT
UNCLASSIFIED	UNCLASSIFIED	UNCLASSIFIED	SAR

Table of Contents

1. INTRODUCTION

The objective of this contract, F 19628-91-K-0013, is to investigate the effect of cell size on bistatic radar clutter statistics due to an elliptically polarized plane wave incident upon a randomly rough surface at 75 degrees. The approach is based on numerical simulation of wave scattering from randomly rough surface using an integral equation method given in the next section. The cases to be studied are summarized in Table 1.

Table 1: Simulation Parameters

Transmitter orientation angle	45 degrees
Transmitter ellipticity angle	30 degrees
Receiver orientation angles	45, 135 degrees
Receiver ellipticity angle	30 degrees
Incident angle	75 degrees
Observation angle	80 degrees
Radar Wavelength (frequency)	18 cm (1.66 GHz)
Scattered azimuthal angles	180, 135, 90, 45, 0 degree
Resolution cells sizes	4, 8, 12 correlation lengths

From Table 1 it is seen that there are two polarizations (like and cross), five azimuthal angles, and three resolution sizes. Thus, the total number of cases is 30. Also of interest is to consider both the statistics of the signal amplitude and those of the signal power. Hence, the total number of cases increases to 60. Following the common practice we shall use the standard statistical models such as Rayleigh, Weibull, Gamma and lognormal to compare with the distributions of the signal amplitude and the corresponding transformed statistical models to compare with the distributions of the signal power. For ease of reference we shall summarize our approach and computational steps in the next section. This is followed by a list of the standard signal distribution functions and their transforms in Section 3. The expected effect of polarization on the mean signal is discussed in Section 4. A special method to estimate the signal distribution function is given in Section 5. Results for last 18 cases are shown in Section 6.

2. APPROACH

The basic approach to study signal statistics is by computer simulation. At this time the most effective method to calculate the scattered field from a three dimensionally rough surface is to determine the surface current at each point on the surface by solving the

integral equation for the surface current, $\vec{J}(\vec{r})$, on a perfectly conducting surface.

$$\vec{J}(\vec{r}) = 2\hat{n} \times \vec{H}_i + \frac{1}{2\pi}\int \hat{n} \times [\nabla G \times \vec{J}(\vec{r}')]\, ds' \tag{1}$$

where $\hat{n}$ is the unit normal vector to the surface and $\vec{H}_i$ is the incident magnetic field. Once the surface current density with p-polarization is known over a surface patch of size A_0 the q-polarized far zone scattered field can be computed from

$$\hat{q} \cdot \vec{E}(\vec{r}) = E_{qp} = -C\eta \hat{q} \cdot \hat{r} \times \int_{A_0} \hat{r} \times \vec{J}_p(\vec{r}') \exp(jk\hat{r} \cdot \vec{r})\, dxdy \tag{2}$$

where C = (-jk/4πR) exp(-jkR), R is range, $\hat{r}$ is the unit vector pointing in the direction of observation, A_0 is the cell size, η is the intrinsic impedance of free space, $\vec{J}_p$ is equal to either $\vec{J}_v$ or $\vec{J}_h$ for vertical and horizontal polarizations respectively, and k is the wave number. The magnitude of the electric field in (2) gives one sample of the scattered field.

To find the surface current density at a point within a cell size of n x m, equation (1) is solved approximately by using the Kirchhoff current density as the estimate of the unknown current density inside the integral [Fung and Chen, 1992]. This operation is carried out for each surface point and, hence, n x m integrations are performed over the cell. Then, equation (2) is used to find the far zone scattered field. Unlike a linearly polarized case, in general all four surface scattering matrix elements, i.e. vertical-vertical, horizontal-horizontal, vertical-horizontal, horizontal-vertical, have to be computed to realize an elliptical polarization. This takes almost four times as much effort in calculations as compared to a single linear polarization.

To carry out the above calculations it is necessary to have a rough surface. For the proposed study an anisotropically rough surface has been generated on the computer. Its surface height statistics are Gaussian and its autocorrelation function is anisotropic with different correlation lengths along two orthogonal directions.The surface rms height is 0.86 cm and and its correlation lengths along orthogonal directions are 6.97 cm and 9.3 cm. Its height distribution and correlation function are illustrated in Figures 1 and 2. In summary, the steps to be taken are as follows:

1. Generate a random surface on the computer with specified height and correlation function.

2. Define the cell size in terms of the number of correlation lengths.

3. For each cell size, frequency, incident and scattered angles, calculate 1100 samples for each of the four elements of the scattering matrix in bistatic scattering and each of the three elements needed in backscattering. Then, evaluate the scattered field amplitude for a desired pair of incident and scattered polarization states (the first choice will be two elliptically polarized
orthogonal polarization states) in terms of the matrix elements and form a probability distribution curve.

4. Compare the calculated distribution curve with Weibull, Gamma distribution, log-normal and Rayleigh functions to find out which analytic function gives the closest description to the distribution. For ease of reference a summary of the properties of these distribution functions are given in Section 3.

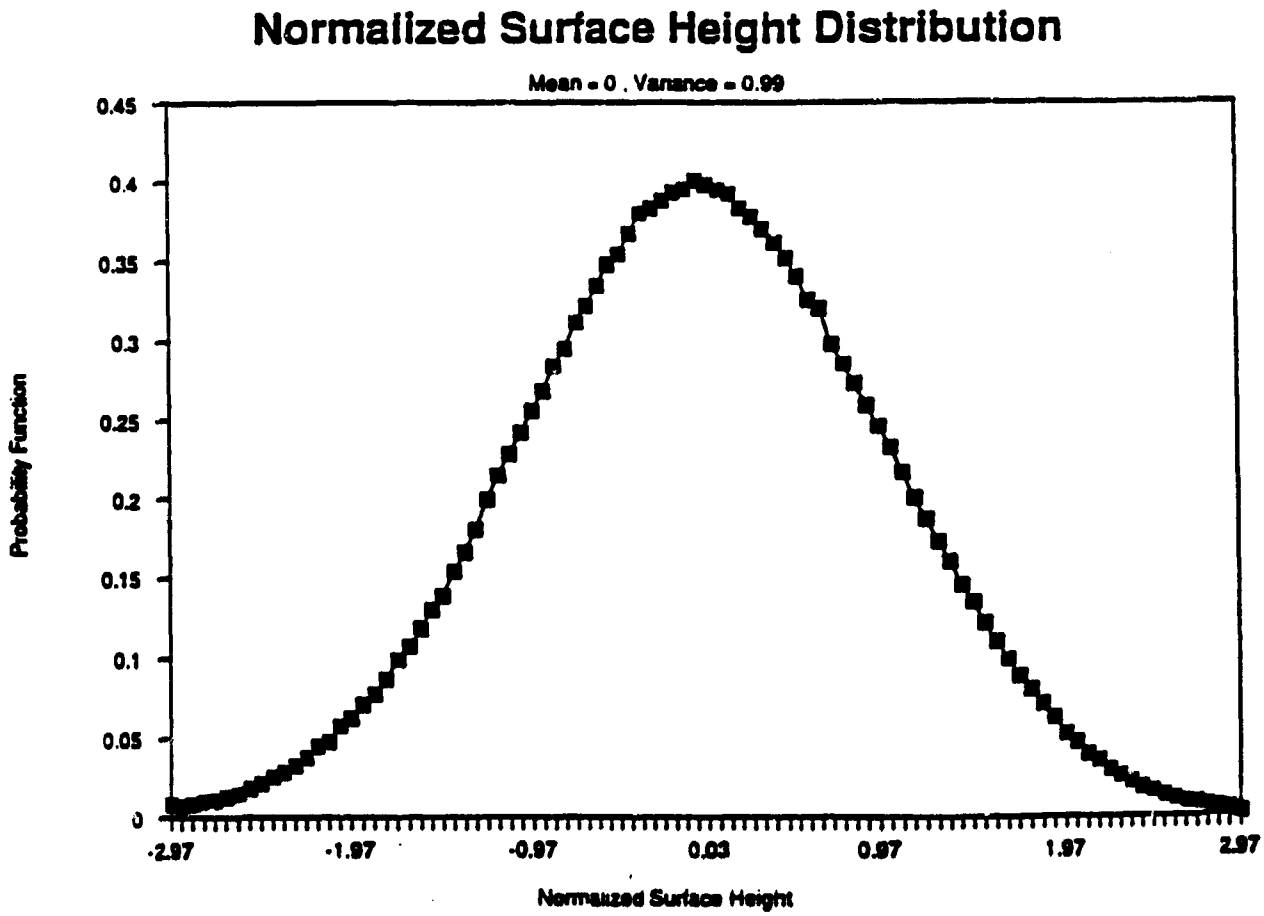

Figure 1 Surface Height Density Function

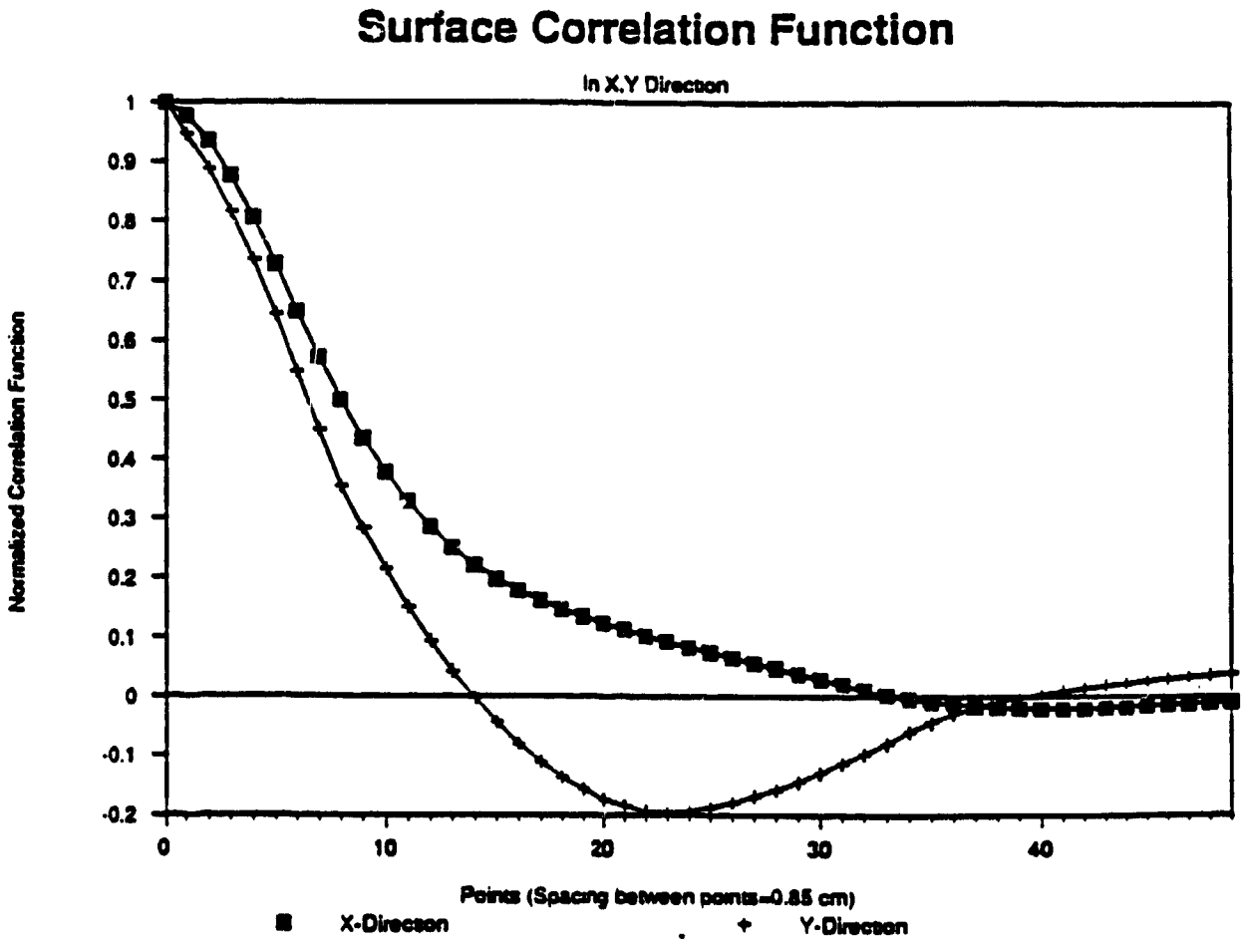

Figure 2 Surface Correlation Function

3. SIGNAL DISTRIBUTION FUNCTIONS

The basic properties of the probability density functions to be used for comparisons with simulated signal distributions are summarized below. Distribution functions listed for the signal amplitude are the standard Rayleigh, Weibull, Gamma and lognormal function. Those for power are the corresponding transformed functions derived from probability theory.

Let x be the envelope of the received field amplitude and y be the corresponding received power where $y = x^2$, then the probability density functions for x and y are defined in the following equations. Note that all model parameters are estimated from the mean μ and variance σ^2 of the random variable x.

(a). The Rayleigh and transformed Rayleigh density functions

$$P_R(x) = \frac{x}{\alpha^2} exp\{-\frac{1}{2}\left(\frac{x}{\alpha}\right)^2\} \tag{3}$$

$$P_{TR}(y) = \frac{1}{2\alpha^2} exp\{-\frac{1}{2}\left(\frac{\sqrt{y}}{\alpha}\right)^2\}, y>0 \tag{4}$$

where

$$\alpha = \mu\sqrt{\frac{2}{\pi}} \tag{5}$$

(b). The lognormal and transformed lognormal density functions

$$P_{ln}(x) = \frac{1}{xv\sqrt{2\pi}} exp\{-\frac{1}{2}\left(\frac{lnx - m}{v}\right)^2\} \tag{6}$$

$$P_{Tln}(y) = \frac{1}{2yv\sqrt{2\pi}} exp\{-\frac{1}{2}\left(\frac{ln\sqrt{y} - m}{v}\right)^2\}, y>0 \tag{7}$$

The parameter m and v can be related to the mean μ and variance σ^2 of x as

$$m = \frac{1}{2} ln\left(\frac{\mu^4}{\sigma^2 + \mu^2}\right) \tag{8}$$

$$v = \sqrt{ln\left(\frac{\sigma^2}{\mu^2}\right)} \tag{9}$$

(c). The Gamma and transformed Gamma density functions

$$P_G(x) = \frac{1}{\alpha\Gamma(\lambda)}\left(\frac{x}{\alpha}\right)^{\lambda-1} exp\left(-\frac{x}{\alpha}\right) \tag{10}$$

$$P_{TG}(y) = \frac{1}{2\alpha\sqrt{y}\Gamma(\lambda)}\left(\frac{\sqrt{y}}{\alpha}\right)^{\lambda-1} exp\left(-\frac{\sqrt{y}}{\alpha}\right) \tag{11}$$

where $\Gamma(x)$ is Gamma function, α is a scale parameter and λ is a shape parameter given by

$$\lambda = \frac{\mu^2}{\sigma^2} \tag{12}$$

$$\alpha = \frac{\sigma^2}{\mu} \tag{13}$$

(d). The Weibull and transformed Weibull density functions

$$P_W(x) = \frac{\lambda}{\alpha}\left(\frac{x}{\alpha}\right)^{\lambda-1} exp\left\{-\left(\frac{x}{\alpha}\right)^{\lambda}\right\} \tag{14}$$

$$P_{TW}(y) = \frac{\lambda}{2\alpha\sqrt{y}}\left(\frac{\sqrt{y}}{\alpha}\right)^{\lambda-1} exp\left\{-\left(\frac{\sqrt{v}}{\alpha}\right)^{\lambda}\right\} \tag{15}$$

where α and λ are scale and shape parameters, respectively, related to the mean and variance of x as (16)

$$\mu = \alpha\Gamma\left(1+\frac{1}{\lambda}\right) \tag{17}$$

$$\sigma^2 = \alpha^2\left[\Gamma\left(1+\frac{2}{\lambda}\right) - \Gamma^2\left(1+\frac{1}{\lambda}\right)\right] \tag{18}$$

Note that to obtain the necessary model parameters from mean and variance one may apply standard algorithms [Gerald and Wheatly, 1984] to solve the nonlinear equations (17) and (18)

4. EFFECTS OF POLARIZATION STATES

In a previous report [Fung, 1990] we discussed signal characteristics of linearly polarized waves scattered from a randomly rough surface. In this section the scattering properties of

plane waves at other polarization states are considered to provide a reference on the average signal property which is an important input parameter to the study of signal distribution considered in this report.

A standard method to denote the polarization state of a plane wave is to use the polarization ellipse defined in terms of the ellipticity angle τ and a pair of orthogonal vector basis, $\hat{x}$ and $\hat{y}$. That is,

$$\vec{E} = (\hat{x}\cos\tau + j\hat{y}\sin\tau)\, E_o exp\,[j(\omega t - kz)] \tag{19}$$

For simplicity we shall set the field amplitude E_o to unity and generalize the polarization state by assuming that the major axis of the ellipse in $\hat{x}$ direction is oriented at an angle ψ from the $\hat{\theta}$ axis of the reference coordinates $\hat{\phi}$ and $\hat{\theta}$ of the transmitting antenna defined in Figure 3. Thus, the polarization state of the transmitting antenna is defined by its radiating field $\vec{E} = \hat{a}_t E_o exp\,[j(\omega t - kz)]$, where the unit polarization vector is

$$\hat{a}_t = \hat{\theta}(\cos\tau\cos\psi - j\sin\tau\sin\psi) + \hat{\phi}(\cos\tau\sin\psi + j\sin\tau\cos\psi) \tag{20}$$

This unit vector is characterized by the ellipticity angle τ and the orientation angle ψ. It is clear that the polarization state of the receiving antenna can be characterized in a similar way and we shall denote it by $\hat{a}_r$. In general, a different set of ellipticity and orientation angles may associate with the receiving antenna. To find the average received power we need to calculate the received voltage using the scattering matrix of the target which is discussed in the next section.

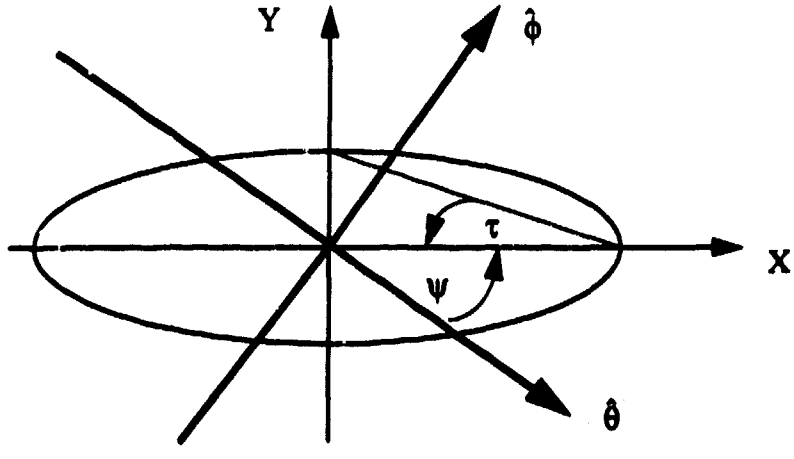

Figure 3 Elliptic polarization state

4.1 Target Scattering Matrix and the Averaged Received Power

The polarization unit vector of the transmitting antenna written in matrix form using phasor representation is

$$\begin{bmatrix} a_{t\theta} \\ a_{t\phi} \end{bmatrix} = \begin{bmatrix} \cos\tau\cos\psi - j\sin\tau\sin\psi \\ \cos\tau\sin\psi + j\sin\tau\cos\psi \end{bmatrix} \tag{21}$$

Let us denote the target scattering matrix by S. That is,

$$S = \frac{e^{-jkR}}{R}\left[S_{qp}\right] = \frac{e^{-jkR}}{R}\begin{bmatrix} S_{\theta\theta} & S_{\theta\phi} \\ S_{\phi\theta} & S_{\phi\phi} \end{bmatrix} \tag{22}$$

and $S_{qp} = exp\,(jkR)\,RE_q^s(\theta_s, \phi_s)/E_p^i(\theta_i, \phi_i)$ where E_p^i and E_q^s denote the incident and scattered fields with polarization states p and q respectively. Then, the normalized received voltage for transmitting polarization t and receiving polarization r is

$$\begin{aligned} V_{rt} &= \frac{e^{-jkR}}{R}\left[a_{r\theta}\ a_{r\phi}\right]\begin{bmatrix} S_{\theta\theta} & S_{\theta\phi} \\ S_{\phi\theta} & S_{\phi\phi} \end{bmatrix}\begin{bmatrix} a_{t\theta} \\ a_{t\phi} \end{bmatrix} \\ &= \left[a_{r\phi}\left(S_{\phi\phi}a_{t\phi} + S_{\phi\theta}a_{t\theta}\right) + a_{r\theta}\left(S_{\theta\phi}a_{t\phi} + S_{\theta\theta}a_{t\phi}\right)\right]\left(e^{-jkR}/R\right) \end{aligned} \tag{23}$$

It is clear that both t and r depend on the ellipticity and orientation angles of the transmitting and receiving antennas respectively. For simplicity we assume that there is no correlation between S_{pq} and S_{pp} or S_{qq}. Then, the expression for the average received power is

$$\begin{aligned} P_{rt} &= \langle |V_{rt}|^2 \rangle \\ &= \Big[|a_{r\phi}|^2\sigma^0_{\phi\phi}|a_{t\phi}|^2 + 2Re\left\{a_{r\phi}a_{r\theta}{}^*\sigma^0_{\phi\phi\theta\theta}a_{t\phi}a_{t\theta}{}^*\right\} + 2Re\left\{a_{r\phi}a_{r\theta}{}^*\sigma^0_{\phi\theta\theta\phi}a_{t\phi}{}^*a_{t\theta}\right\} \\ &\quad + |a_{r\phi}|^2\sigma^0_{\phi\theta}|a_{t\theta}|^2 + |a_{r\theta}|^2\sigma^0_{\theta\phi}|a_{t\phi}|^2 + |a_{r\theta}|^2\sigma^0_{\theta\theta}|a_{t\theta}|^2 \Big] A/(4\pi R^2) \end{aligned} \tag{24}$$

where * is the symbol for complex conjugate; R is the range from the transmitting antenna to the illuminated area A and $\sigma^0_{\phi\theta\theta\phi}$ and $\sigma^0_{\phi\phi\theta\theta}$ are the scattering coefficients defined as follows:

$$\sigma^0_{\phi\theta\theta\phi} = 4\pi\langle S_{\phi\theta}S_{\theta\phi}{}^*\rangle/A$$

$$\sigma^0_{\phi\phi\theta\theta} = 4\pi\langle S_{\phi\phi}S_{\theta\theta}{}^*\rangle/A$$

Note that once the antenna coordinates, θ and ϕ, are fixed, the target scattering matrix

defined in terms of them are fixed irrespective of the choice of the transmitting or receiving antenna polarization state which is a function of the angles τ and ψ. Hence, it is possible to determine the response to different polarization states with a given set of S_{pq}'s which is a function of the incident and scattered directions. It is a common practice to calculate the scattering coefficient rather than the average power which has range dependence. This scattering coefficient which is for elliptic polarization has the form

$$\begin{aligned}\sigma^0_{rt} &= 4\pi R^2 P_{rt}/A \\ &= |a_{r\phi}|^2\sigma^0_{\phi\phi}|a_{t\phi}|^2 + 2Re\,(a_{r\phi}a_{r\theta}{}^*\sigma^0_{\phi\phi\theta\theta}a_{t\phi}a_{t\theta}{}^*) + 2Re\,(a_{r\phi}a_{r\theta}{}^*\sigma^0_{\phi\theta\theta\phi}a_{t\phi}{}^*a_{t\theta}) \\ &+ |a_{r\phi}|^2\sigma^0_{\phi\theta}|a_{t\theta}|^2 + |a_{r\theta}|^2\sigma^0_{\theta\phi}|a_{t\phi}|^2 + |a_{r\theta}|^2\sigma^0_{\theta\theta}|a_{t\theta}|^2. \end{aligned} \tag{25}$$

To do computation with (25) we need to know all the scattering coefficients which appear in it.

For backscattering from a randomly rough surface all the scattering coefficients in (25) are given in Appendix A. The important point to note is that while like polarized scattering is always higher than that of the cross in vertically and horizontally polarized backscattering, this is not necessarily true in elliptical polarization and definitely not true in bistatic scattering into directions orthogonal to the incident in azimuth. In particular, for polarization at 30 degrees ellipticity and 45 degree orientation, the levels of like and cross polarized scattering are of the same order.

Like and Cross Polarizations

Following definitions developed in antenna reception theory [Mott, 1986], we define like polarization to be reception with matched antennas i.e.

$$|\hat{a}_r \cdot \hat{a}_t| = 1 \tag{26}$$

and cross or orthogonal polarization to be with zero reception i.e.

$$|\hat{a}_r \cdot \hat{a}_t| = 0 \tag{27}$$

To illustrate the meaning of (26) consider the case $\psi = 0$. Let (19) represent the radiated wave from a transmitting antenna. Rewriting (19) in time domain with $E_0 = 1$, we have

$$\vec{E}_t = \hat{x}\cos\tau\cos(\omega t - kz) - \hat{y}\sin\tau\sin(\omega t - kz) \tag{28}$$

which is a left-hand elliptically polarized wave. If the receiving antenna is chosen to have the same polarization, its radiated field will have the same mathematical form but expressed in prime coordinates. As illustrated in Figure 4 transmitting and receiving antenna systems must point in opposite directions. This means that when the radiated field

of the receiving antenna is expressed in the coordinate system of the transmitting antenna, its propagation phase must take the form $\omega t + kz$ and there is a sign change on the y-component. That is

$$\vec{E}_r = \hat{x}\cos\tau\cos(\omega t + kz) + \hat{y}\sin\tau\sin(\omega t + kz) \tag{29}$$

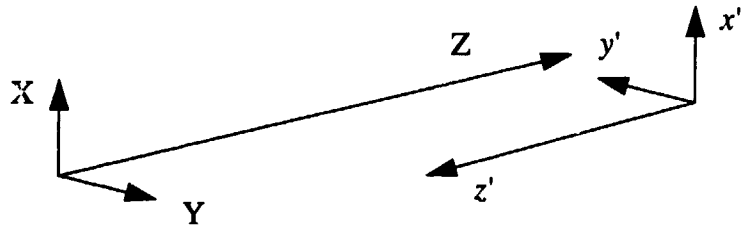

Figure 4 Illustration of transmitting and receiving antenna systems

When we convert (29) to phasor form, it becomes

$$\vec{E}_r = (\hat{x}\cos\tau - j\hat{y}\sin\tau)\, exp\,[j(\omega t + kz)] \tag{30}$$

From (19) and (30) the polarization unit vectors for transmitting and receiving are respectively

$$\hat{a}_t = \hat{x}\cos\tau + j\hat{y}\sin\tau$$

and

$$\hat{a}_r = \hat{x}\cos\tau - j\hat{y}\sin\tau$$

Clearly, one unit vector is the complex conjugate of the other, $|\hat{a}_r \cdot \hat{a}_t| = 1$ and the polarization states of both antennas are left-hand elliptic. Hence, this case is referred to as like polarization.

To illustrate cross or orthogonal polarization consider the transmitting antenna defined by (20) and take the receiving antenna to be the same but rotated 90 degrees in orientation. That is, replace ψ in (20) by $\psi + \pi/2$ yielding

$$\hat{a}_r = \hat{\theta}(-\cos\tau\sin\psi - j\sin\tau\cos\psi) + \hat{\phi}(\cos\tau\cos\psi - j\sin\tau\sin\psi) \tag{31}$$

If we take the dot product of (20) and (31), we find that $\hat{a}_r \cdot \hat{a}_t = 0$. When we check its polarization state, it is right-hand elliptic. Thus, left-hand elliptic and right hand elliptic polarizations are mutually orthogonal. The special case with $\tau = 0$ and $\psi = 0$ leads to $\hat{a}_r = \hat{\phi}$ and $\hat{a}_t = \hat{\theta}$ which are obviously orthogonal.

5. METHOD OF DENSITY ESTIMATION

The most widely used density estimator is the histogram. For the presentation and exploration of data, histograms are of course an extremely useful class of density estimators, particularly in the univariate case. However, this method has some substantial drawbacks such as the discontinuity of the estimate, the choice of origin and the choice of the amount of smoothing. To overcome these shortcomings, we adopt the kernel estimate method [Silverman, 1986] for our data presentation and analysis.

5.1 Kernel Estimator

From the definition of a probability density, if the random variable X has density f, then

$$f(x) = \lim_{h \to 0} \frac{1}{2h} P(x - h < X < x + h) \tag{32}$$

For any given h, we can estimate $P(x - h < X < x + h)$ by the percent of the samples falling in the interval $(x - h, x + h)$. Thus, a natural estimator $\hat{f}$ of the density is given by choosing a small number h and setting

$$\hat{f}(x) = \frac{1}{nh} \sum_{i=1}^{n} \left(\frac{x - X_i}{h} \right) K(x) \tag{33}$$

where K, the kernel, satisfies the conditions

$$\int K(x)\,dx = 1 \tag{34}$$

$$\int xK(x)\,dx = 0 \tag{35}$$

$$\int x^2 K(x)\,dx = c \neq 0 \tag{36}$$

and h is the window width, also called the smoothing parameter or bandwidth, and n is the sample size.Usually, but not always, K will be a symmetric probability density function. Some fundamental properties of kernel estimates follow from the definition. When the kernel K is everywhere non-negative and satisfies the conditions (34)-(36)-in other words is a probability density function-it will follow from the definition that $\hat{f}$ will itself be a probability density function. Furthermore, $\hat{f}$ will inherit all the continuity and differentiability properties of the kernel K. For example, if K is a normal density function, then $\hat{f}$ will be a smooth curve having derivatives of all orders.

5.2 Ideal Window Width and Kernel

The ideal value of h may be found from the point of view of minimizing the approximate mean integrated square error leading to

$$h_{opt} = c^{-2/5} n^{-1/5} \{\int K(x)^2 dx\}^{1/5} \{\int f''(x)^2 dx\}^{-1/5} \tag{37}$$

The equation above for the optimal window width is somewhat disappointing since it shows that h_{opt} itself depends on the unknown density being estimated. However, some informative conclusions can be draw. Firstly, the ideal window width will converge to zero as the sample size increase, but at a very slow rate. Secondly, since the second integral term in (37) measures, in a sense, the rapidity of fluctuations in the density f, it can be seen that smaller values of h will be appropriate for more rapidly fluctuating densities. A very easy and natural way is to use a standard family of distribution to assign a value to the second integral term in Eq. (37) for the optimal window width. Silverman [1986] suggests that if data come from a unimodal distribution, then for a Gaussian kernel the choice,

$$h = 1.06\sigma n^{-1/5} \tag{38}$$

will, to a high degree of accuracy, minimize the integrated mean square error with an estimate of σ obtained from the data. For multimodal populations this choice may cause some oversmoothing.

5.3 Method of Computation

Both theory and practice [Silverman, 1986] suggest that the choice of kernel is not crucial to the statistical performance of the method and therefore it is quite reasonable to choose a kernel for computational efficiency. The kernel we shall use is the standard Gaussian density function. The numerical method used is first to discretize the data to a very fine grid, and then to use the FFT to convolve the data with the kernel to obtain the estimate. Take Fourier transforms in (33) to obtain

$$f_n(s) = \sqrt{(2\pi)}\,\tilde{K}(hs)\,y(s) \tag{39}$$

where $y(s)$,$\tilde{K}$ are the Fourier transforms of the data and kernel, respectively.

$$y(s) = (2\pi)^{-0.5} n^{-1} \sum_{i=1}^{n} exp(isX_i) \tag{40}$$

Next, substitute the Fourier transform of the Gaussian kernel to obtain

$$\tilde{f}_n(s) = exp\left(-\frac{1}{2}h^2 s^2\right) y(s) \tag{41}$$

A discrete approximation to *y(s)* is found by constructing a histogram on a grid of 2^k cells and then applying the FFT. Finally, $f_n(x)$ is found by taking the inverse Fourier transform of (41). Note that because of rounding and approximation errors, this calculation may lead to some (numerically very small) negative values of $f_n(x)$. These are set to zero.

6. RESULTS

Figures 5.1a through 5.1c show the signal distribution curves calculated from simulated data along with distribution functions given in Section 3 for small (4L), medium (8L) and large cell (12L) sizes respectively (where L is surface correlation length) for a receiving orientation angle of 45 degrees and azimuthal angle of ϕ_s = 90 degrees. In each figure the upper graph is the distribution for signal amplitude and the lower graph is for the distribution of power.The corresponding rms error calculations for the different distribution functions are shown in Tables 5a,b,c. From Figure 5a, it is seen that none of the common distribution functions fit the simulated data very well when the cell size is small. As cell size increases to the size shown in Figure 5b, much better agreement is obtained between the data and Weibull distribution for the signal amplitude. However, when the same data set is analyzed in terms of power, the agreement is not as good although the transformed Weibull density is still the best among those considered. The reason for this is because the squaring operation compresses all signal values that are small and spreads out those that are large. The end result is that finer resolution is needed in the small value region and a coarser resolution in the large value region. Thus, *to analyze signal properties on the voltage instead of the power level generally produces better defined curves.* Further increase in the cell size leads to similar conclusions and a better agreement between the data and the Weibull distribution. In fact, the rms error decreases from 0.697 for the small cell size to 0.215 for the large cell size using voltage calculations. Another point to note is that for large cell size (Figure 5c), the power data and the common distribution functions have a long, exponential tail in the region exceeding the mean and in this tail region the difference between distributions is very

small. This again indicates that the use of data on the power level for analysis loses sensitivity to the true curve. Thus, *the well known Rayleigh distribution can be used for signal distribution on the power level when one deals only with the tail region.*

Similar illustrations for an azimuthal angle of 45 degrees are shown in Figures 6a through 6c and the associated error analysis is summarized in Table 6a,b,c. In all cases Weibull distribution comes closest to the simulated data. Unlike the case with an azimuthal angle of 90, an increase in cell size causes an increase in rms error from 0.204 to 0.529 in error analysis. Visually, it is still the large cell size that leads to a better agreement in the shape of the curve. In all cases the Gamma distribution is the second best descriptor. Another point worthy of notice is that unlike those cases where the azimuthal angle is larger than or equal to 90, the power curves do not have an exponential appearance over a significant portion of their range until the cell size is large. This means that the use of Rayleigh distribution in practice for the tail region (power value larger than the mean) is justified only when the cell size is large.

When the azimuthal angle is 0 degree(i.e. in the forward direction), the *shape* of the signal distribution curve shifts over to Gamma, although the rms error for Weibull distribution is still the smallest. Illustrations are given in Figures 7a through 7c and Tables 7a,bc. Here, again it is the largest cell size that produces the best agreement and the least amount of error. In addition, on the power level, the curves appear more symmetric especially for larger cell sizes and lose their exponential appearance completely. Thus, in forward direction the common practice of assuming Rayleigh distribution is completely invalid.

7. CONCLUSIONS

1. The signal distribution is found to have a closer correlation to target when the signal envelop rather than signal power is used for analysis.
2. Away from the forward direction and for signal levels larger than the mean, Rayleigh distribution can be used to estimate power distribution even though the actual distribution curve is not Rayleigh.
3. Away from the forward direction Weibull distribution gives the closest description of the signal distribution.
4. In the forward direction the Gamma distribution gives a closer description of the shape of the distribution curve.

8. REFERENCE

Fung, A.K., Effect of cell size on radar clutter statistics, RADC-TR-90-235, September, 1990

Fung, A.K and K.S. Chen, *Bistatic Signal Statistics of Randomly Rough Surfaces*, IEEE IGARSS' 92 Symposium.,

Gerald, C. F. and P. O. Wheatley, *Applied Numerical Analysis*, Addison-Wesley, Reading, MA,1984.

Mott, H., Polarization in antennas and radar, John Wiley and Sons, 1986

Silverman, B. W., *Density Estimation for Statistics and Data Analysis*, Chapman & Hall, New York, NY, 1986.

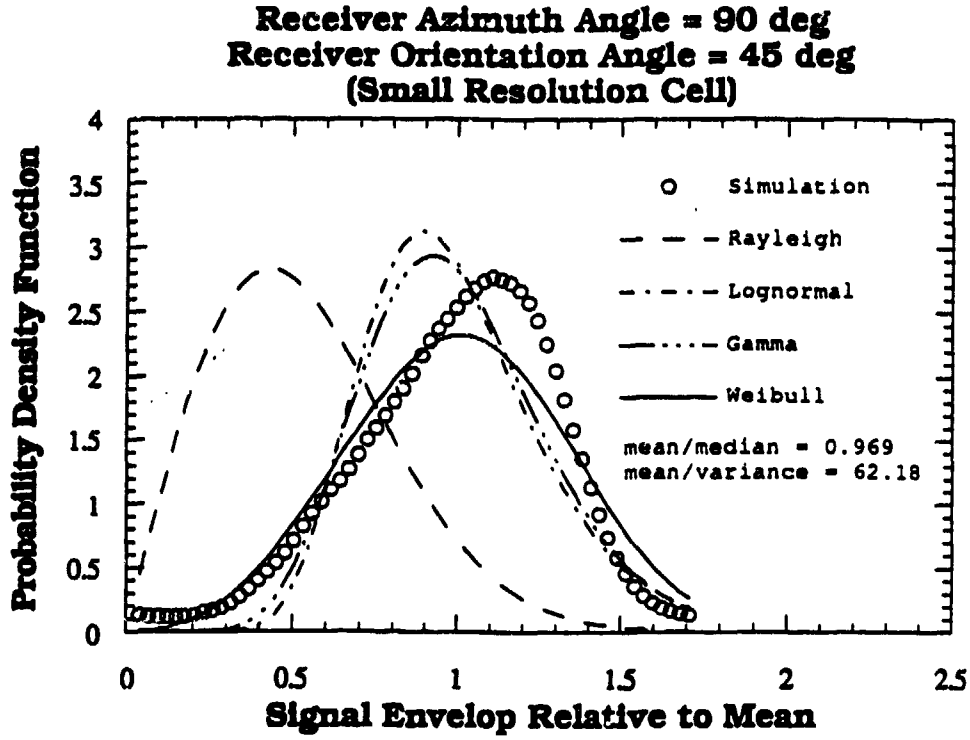

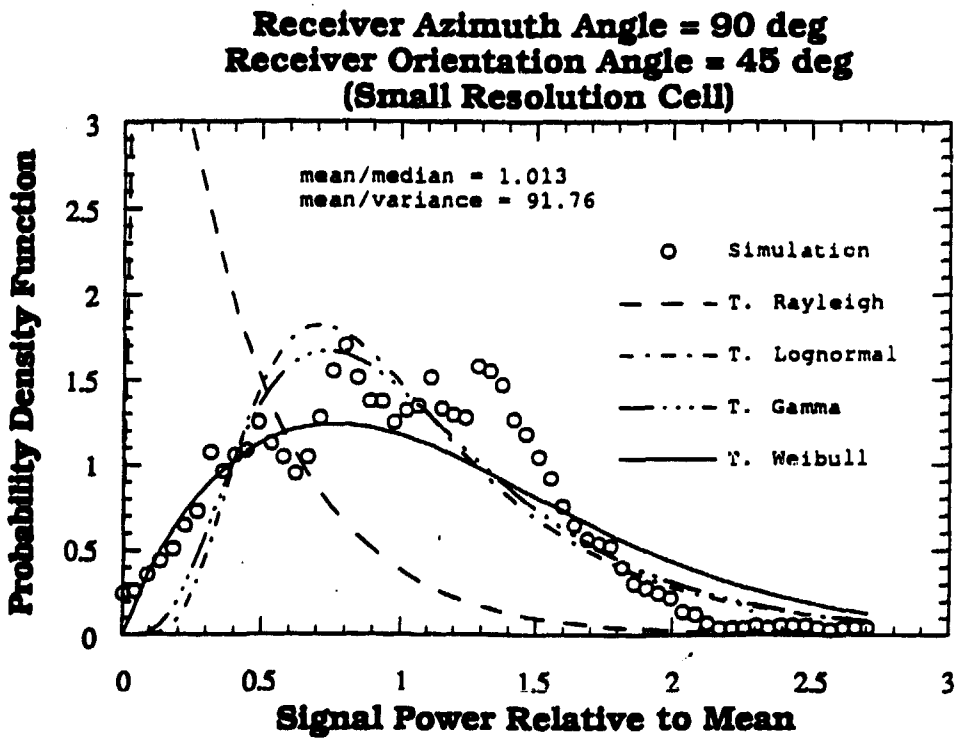

Figure 5a. Comparison between statistical models and simulated data for the small cell size.

Table 5a

Signal Envelope

Model	RMS Error	Model Parameters	
		shape	scale
Rayleigh	3.930		0.9
Lognormal	1.201	-1.63	0.28
Gamma	0.884	12.1	0.017
Weibull	0.697	3.26	0.23
mean= 2.0e-1		variance=3.4e-3	

Signal Power

Model	RMS Error	Model Parameters	
		shape	scale
T. Rayleigh	9.853		0.9
T. Lognormal	3.977	-1.63	0.28
T. Gamma	3.674	12.1	0.017
T. Weibull	3.267	3.26	0.23
mean=4.5e-2		variance= 4.9e-4	

Small Resolution Cell

Cell Size = 4 Correlation Lengths

$\tau_t = \tau_s = 30$ Deg., $\theta_i = 75$ Deg., $\theta_s = 80$ Deg.,

$\psi_t = 45$ Deg., $\psi_s = 45$ Deg., $\phi_s = 90$ Deg.

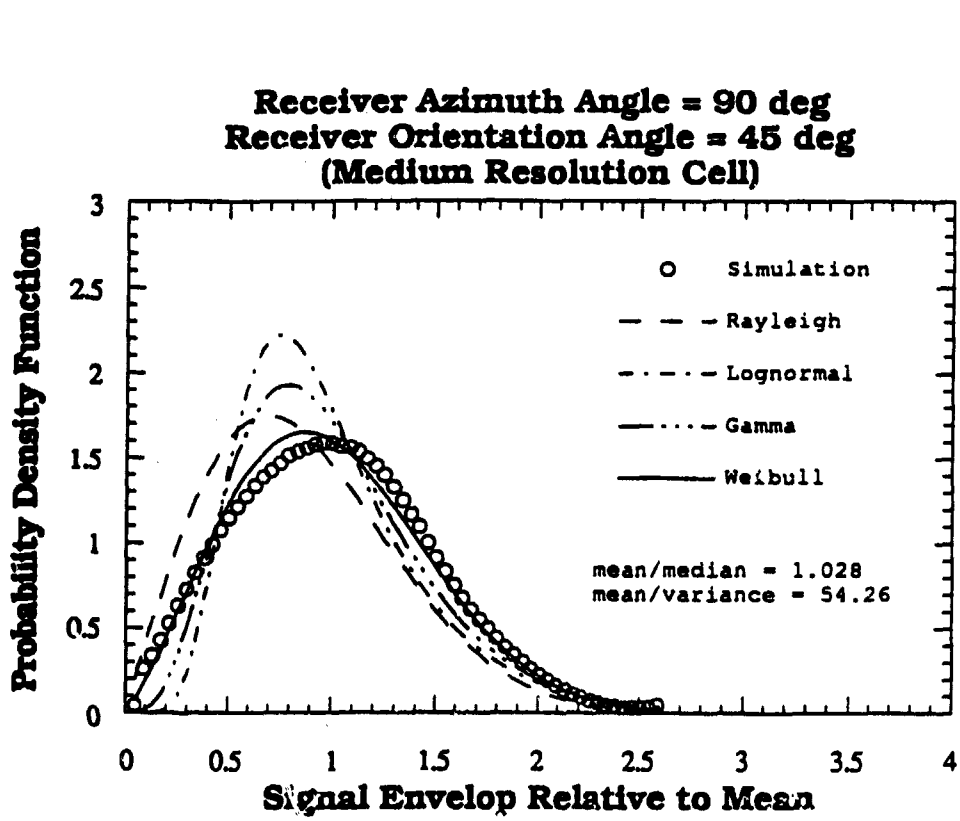

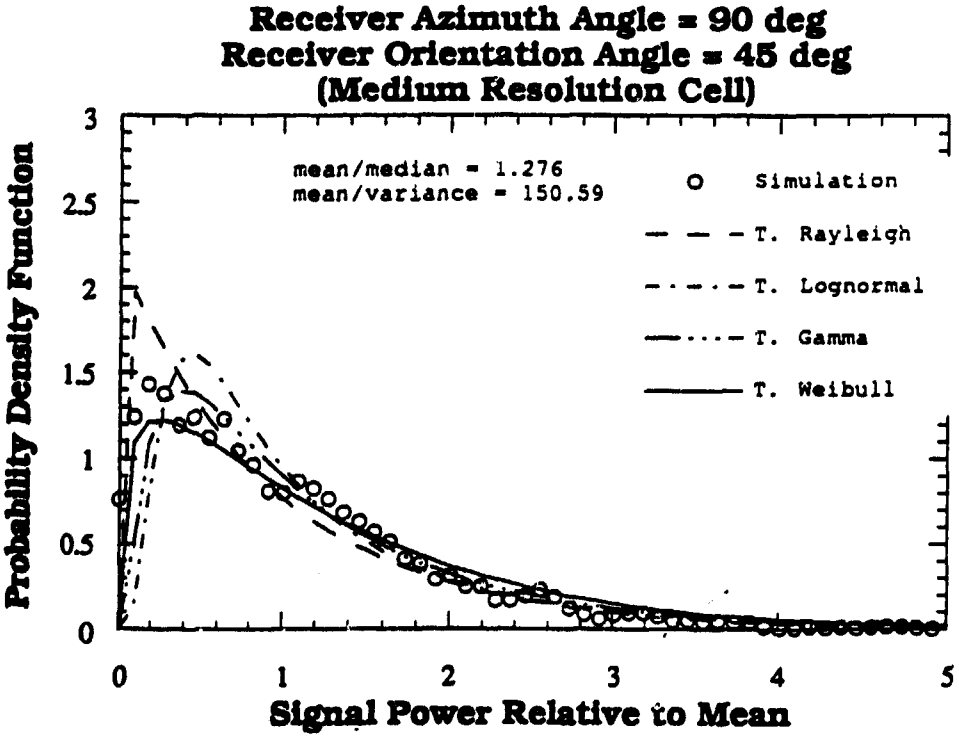

Figure 5b. Comparison between statistical models and simulated data for the medium cell size.

Table 5b

Signal Envelope

Model	RMS Error	Model Parameters	
		shape	scale
Rayleigh	1.241		0.063
Lognormal	1.327	-2.51	0.44
Gamma	0.631	4.76	0.019
Weibull	0.375	2.25	0.10
mean= 9.0e-2		variance=1.7e-3	

Signal Power

Model	RMS Error	Model Parameters	
		shape	scale
T. Rayleigh	7.641		0.063
T. Lognormal	7.770	-2.51	0.44
T. Gamma	5.126	4.76	0.019
T. Weibull	4.397	2.25	0.10
mean=9.6e-3		variance=6.3e-5	

Medium Resolution Cell

Cell Size = 8 Correlation Lengths

$\tau_t = \tau_s = 30$ Deg., $\theta_i = 75$ Deg., $\theta_s = 80$ Deg.,

$\Psi_t = 45$ Deg., $\Psi_s = 45$ Deg., $\phi_s = 90$ Deg.

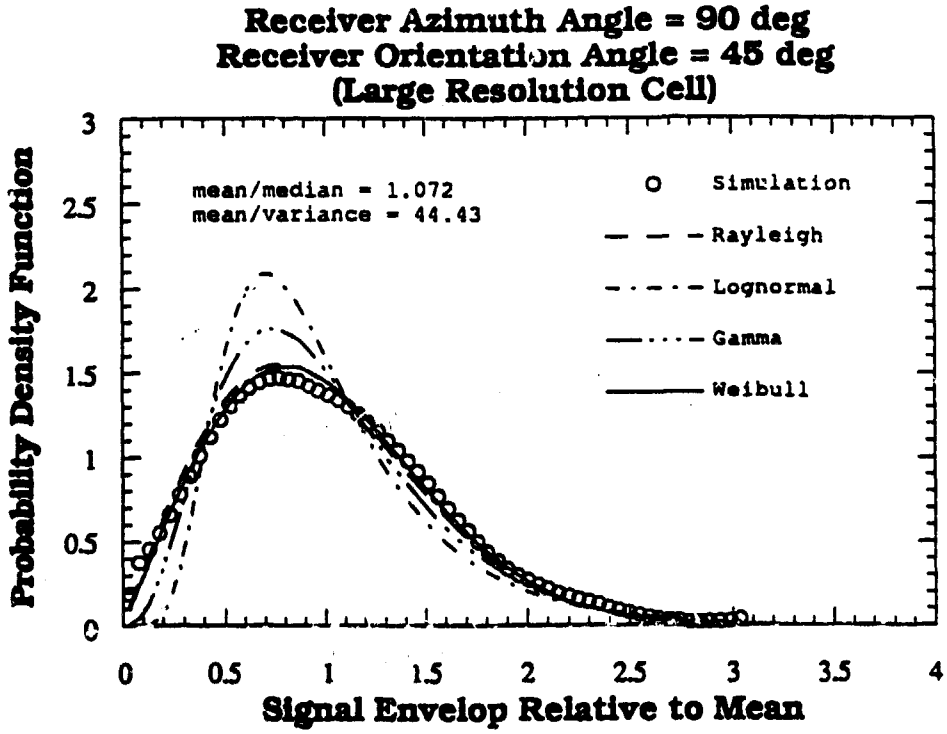

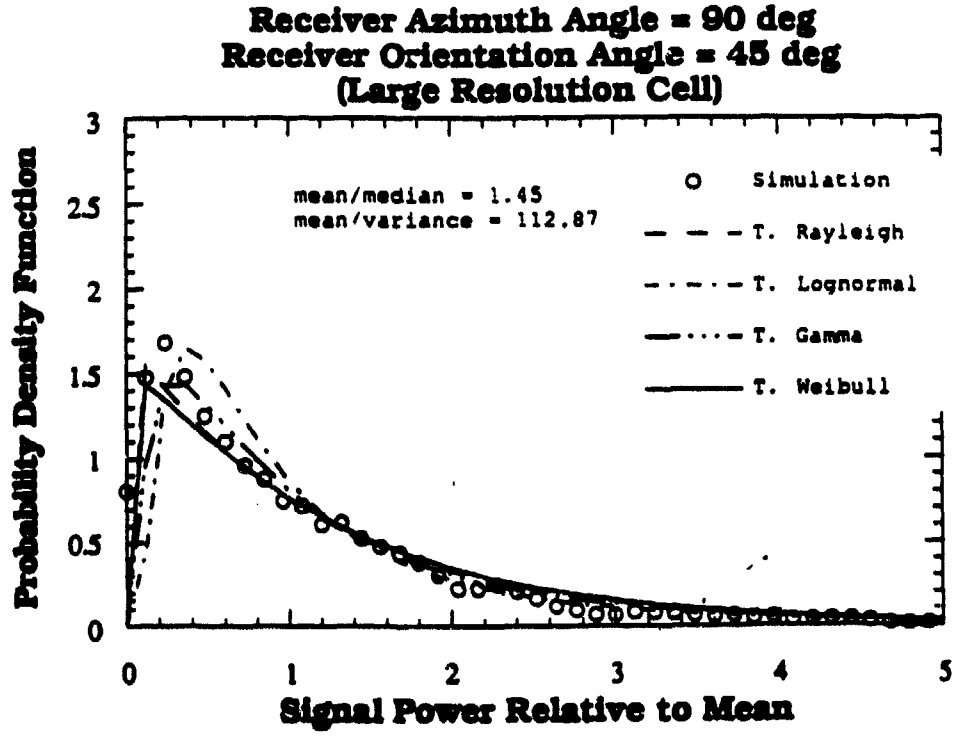

Figure 5c. Comparison between statistical models and simulated data for the large cell size.

Table 5c

Signal Envelope

Model	RMS Error	Model Parameters	
		shape	scale
Rayleigh	0.314		0.068
Lognormal	1.276	-2.57	0.49
Gamma	0.849	3.71	0.023
Weibull	0.215	1.98	0.098
mean= 8.6e-2		variance=2.0e-3	

Signal Power

Model	RMS Error	Model Parameters	
		shape	scale
T. Rayleigh	2.889		0.068
T. Lognormal	5.217	-2.57	0.49
T. Gamma	4.096	3.71	0.023
T. Weibull	2.651	1.98	0.098
variance=8.2e-5			

Large Resolution Cell

Cell Size = 12 Correlation Lengths

$\tau_t = \tau_s = 30$ Deg., $\theta_i = 75$ Deg., $\theta_s = 80$ Deg.,

$\Psi_t = 45$ Deg., $\Psi_s = 45$ Deg., $\phi_s = 90$ Deg.

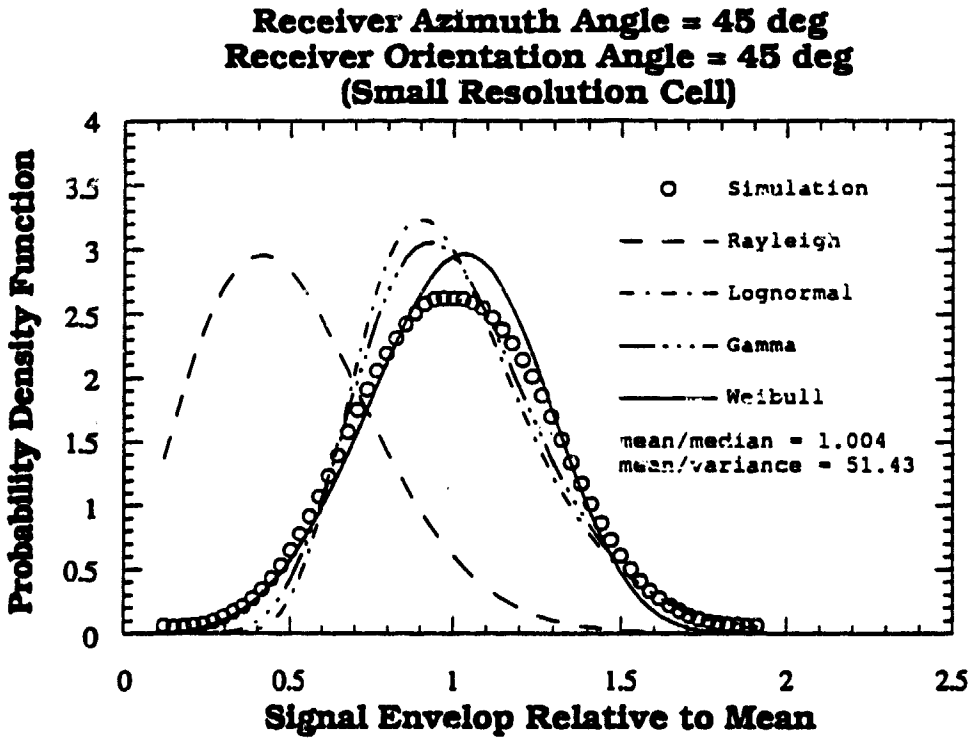

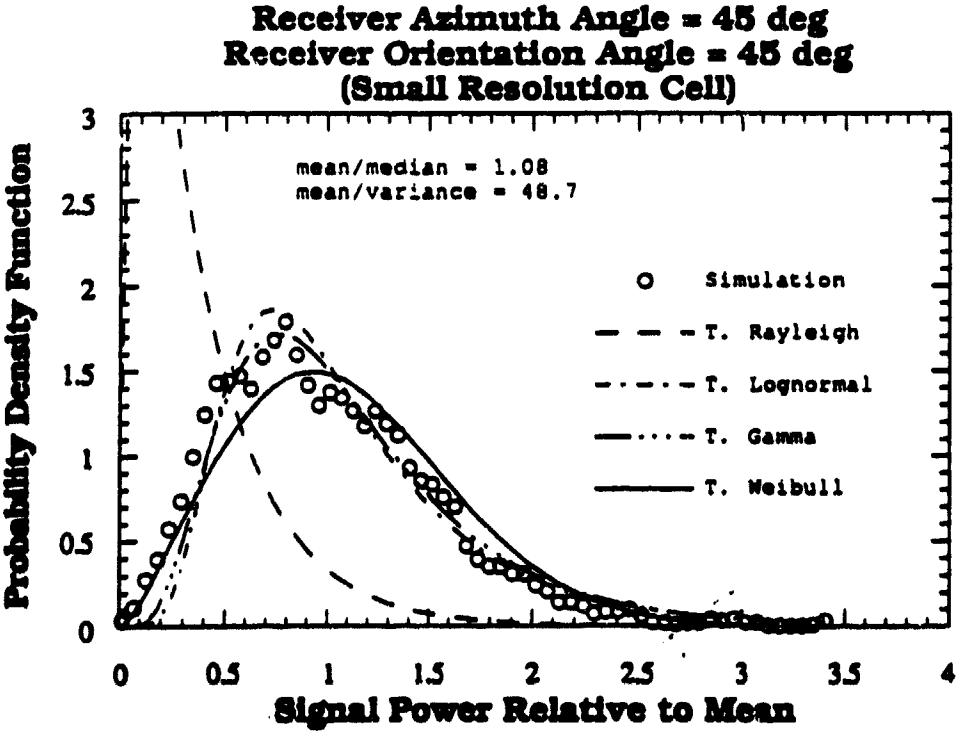

Figure 6a. Comparison between statistical models and simulated data for the small cell size.

Table 6a

Signal Envelope

Model	RMS Error	Model Parameters	
		shape	scale
Rayleigh	2.875		0.11
Lognormal	0.777	-1.35	0.27
Gamma	0.521	13.0	0.021
Weibull	0.204	4.11	0.3
mean= 2.7e-1		variance=5.6e-3	

Signal Power

Model	RMS Error	Model Parameters	
		shape	scale
T. Rayleigh	4.529		0.11
T. Lognormal	1.334	-1.35	0.27
T. Gamma	1.268	13.0	0.021
T. Weibull	0.793	4.11	0.3
mean=7.8e-2		variance=1.6e-3	

Small Resolution Cell

Cell Size = 4 Correlation Lengths

$\tau_t = \tau_s = 30$ Deg., $\theta_i = 75$ Deg., $\theta_s = 80$ Deg.,

$\Psi_t = 45$ Deg., $\Psi_s = 45$ Deg., $\phi_s = 45$ Deg.

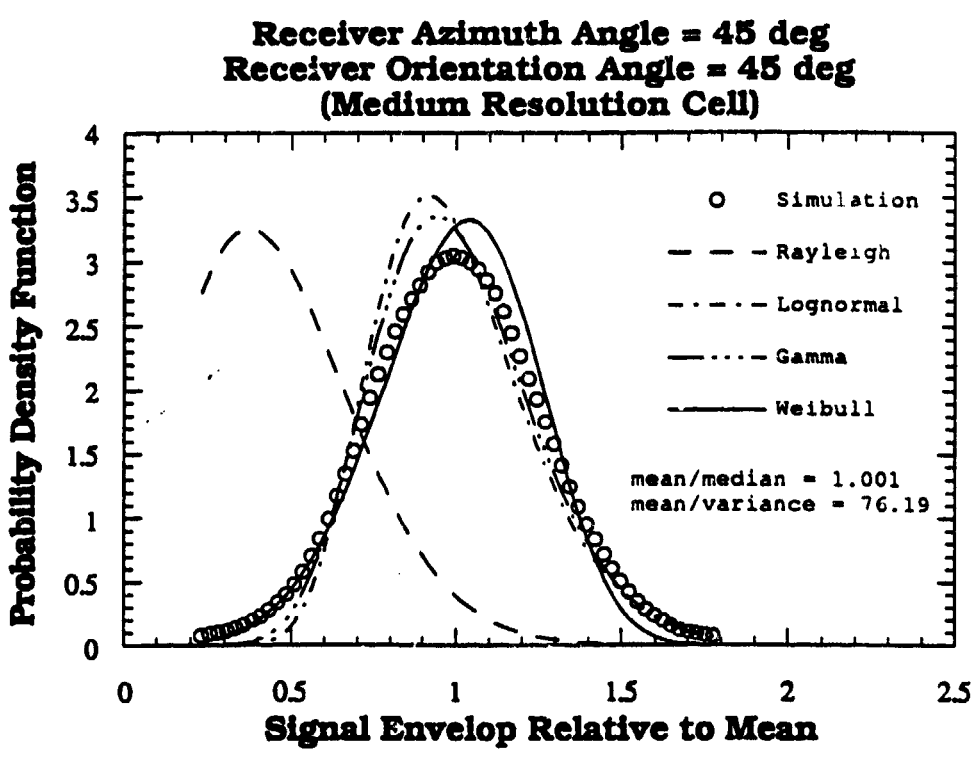

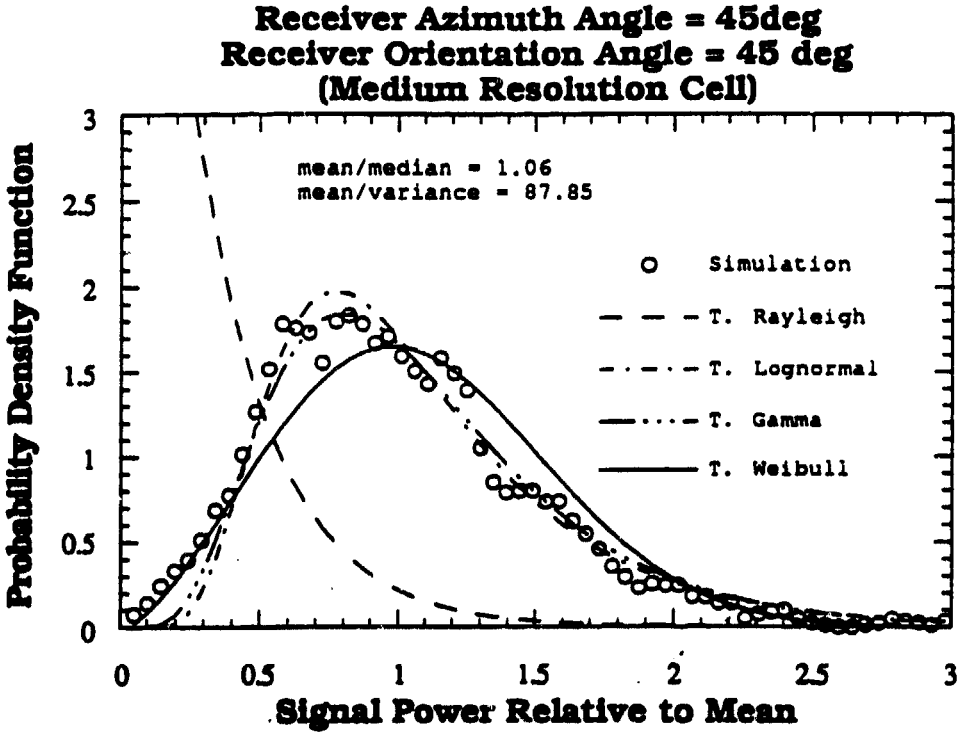

Figure 6b. Comparison between statistical models and simulated data for the medium cell size.

Table 6b

Signal Envelope

Model	RMS Error	Model Parameters	
		shape	scale
Rayleigh	3.766		0.084
Lognormal	0.409	-1.54	0.25
Gamma	0.335	16.1	0.014
Weibull	0.287	4.69	0.24
mean= 2.2e-1		variance=3.0e-3	

Signal Power

Model	RMS Error	Model Parameters	
		shape	scale
T. Rayleigh	9.341		0.084
T. Lognormal	2.354	-1.54	0.25
T. Gamma	2.030	16.1	0.014
T. Weibull	1.694	4.69	0.24
mean=5.1e-2		variance=6.0e-4	

Medium Resolution Cell

Cell Size = 8 Correlation Lengths

$\tau_t = \tau_s = 30$ Deg., $\theta_i = 75$ Deg., $\theta_s = 80$ Deg.,

$\Psi_t = 45$ Deg., $\Psi_s = 45$ Deg., $\phi_s = 45$ Deg.

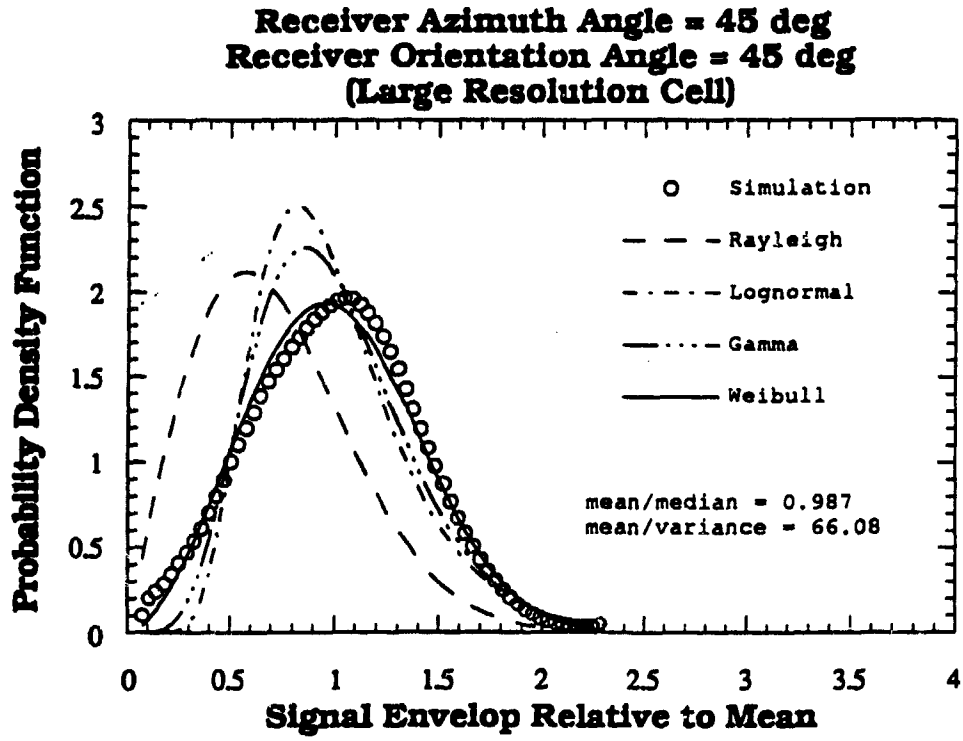

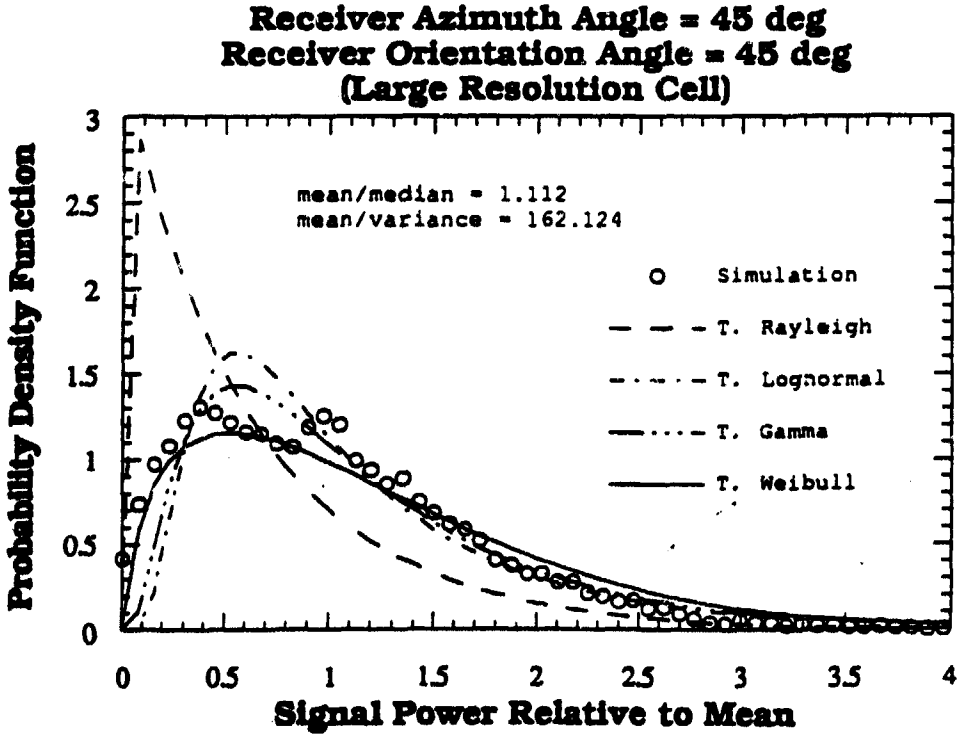

Figure 6c. Comparison between statistical models and simulated data for the large cell size.

Table 6c

Signal Envelope

Model	RMS Error	Model Parameters	
		shape	scale
Rayleigh	2.851		0.063
Lognormal	1.352	-2.3	0.37
Gamma	1.046	6.85	0.016
Weibull	0.529	2.67	0.12
mean= 1.1e-1		variance=1.7e-3	

Signal Power

Model	RMS Error	Model Parameters	
		shape	scale
T. Rayleigh	11.30		0.063
T. Lognormal	6.317	-2.3	0.37
T. Gamma	4.449	6.85	0.016
T. Weibull	3.694	2.67	0.12
mean=1.3e-2		variance=8.0e-5	

Large Resolution Cell

Cell Size = 12 Correlation Lengths

$\tau_t = \tau_s = 30$ Deg., $\theta_i = 75$ Deg., $\theta_s = 80$ Deg.,

$\Psi_t = 45$ Deg., $\Psi_s = 45$ Deg., $\phi_s = 45$ Deg.

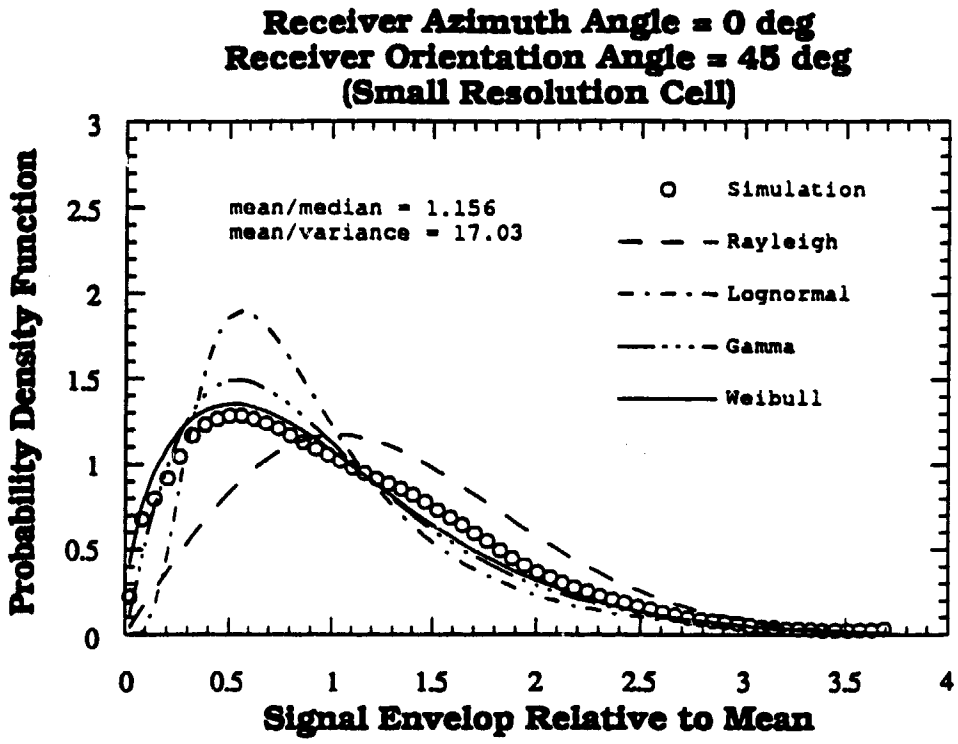

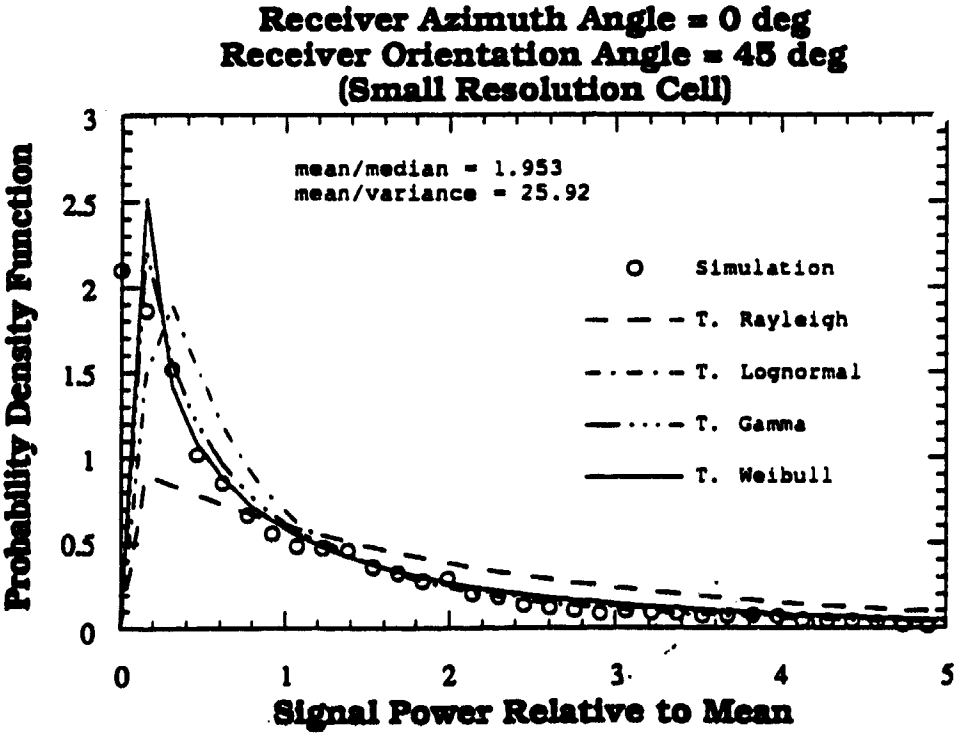

Figure 7a. Comparison between statistical models and simulated data for the small cell size.

Table 7a

Signal Envelope

Model	RMS Error	Model Parameters	
		shape	scale
Rayleigh	0.764		0.13
Lognormal	0.655	-2.21	0.60
Gamma	0.246	2.31	0.057
Weibull	0.137	1.55	0.15
mean= 1.3e-1		variance=7.5e-3	

Signal Power

Model	RMS Error	Model Parameters	
		shape	scale
T. Rayleigh	1.942		0.13
T. Lognormal	1.229	-2.21	0.60
T. Gamma	1.037	2.31	0.057
T. Weibull	0.854	1.55	0.15
mean=2.3e-2		variance=9.2e-4	

Small Resolution Cell

Cell Size = 4 Correlation Lengths

$\tau_t = \tau_s = 30$ Deg., $\theta_i = 75$ Deg., $\theta_s = 80$ Deg.,

$\psi_t = 45$ Deg., $\psi_s = 45$ Deg., $\phi_s = 0$ Deg.

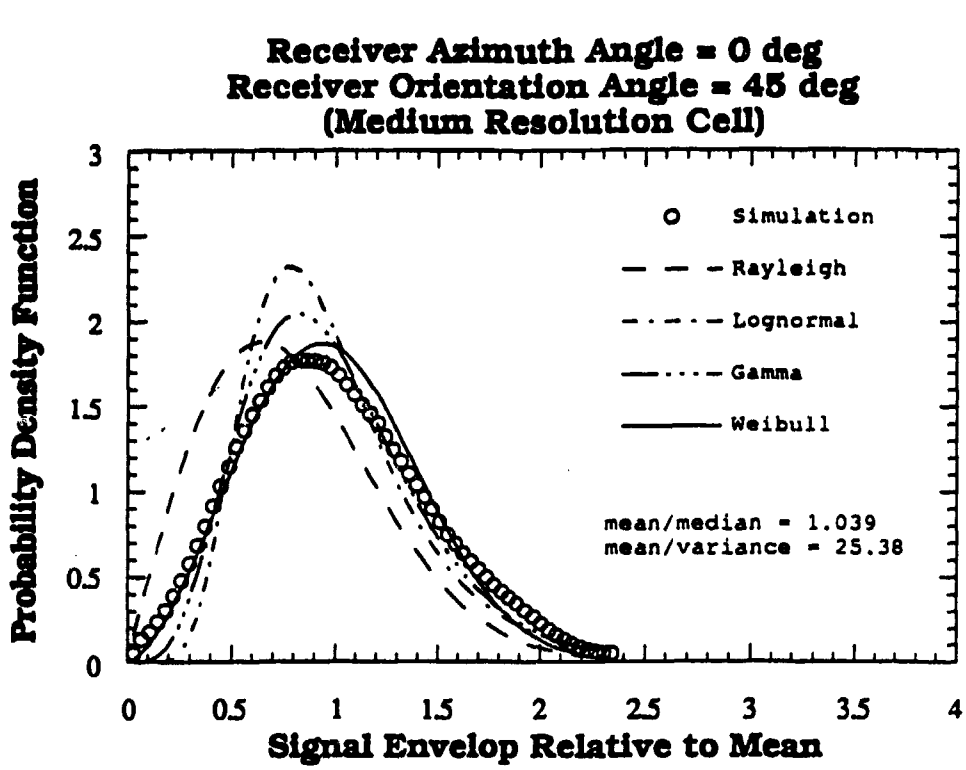

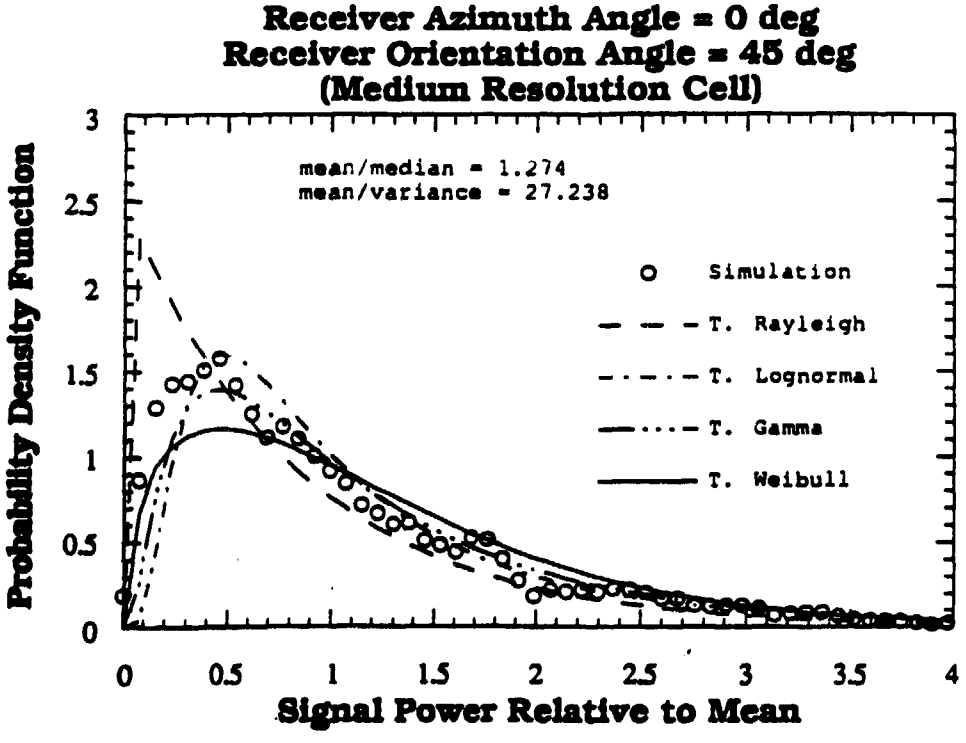

Figure 7b. Comparison between statistical models and simulated data for the medium cell size.

Table 7b

Signal Envelope

Model	RMS Error	Model Parameters	
		shape	scale
Rayleigh	0.745		0.14
Lognormal	0.576	-1.60	0.41
Gamma	0.226	5.37	0.041
Weibull	0.175	2.52	0.25
mean= 2.2e-1		variance= 9.0e-3	

Signal Power

Model	RMS Error	Model Parameters	
		shape	scale
T. Rayleigh	1.587		0.14
T. Lognormal	1.125	-1.60	0.41
T. Gamma	0.997	5.37	0.041
T. Weibull	0.715	2.52	0.25
mean=5.7e-2		variance=2.1e-3	

Medium Resolution Cell

Cell Size = 8 Correlation Lengths

$\tau_t = \tau_s = 30$ Deg., $\theta_i = 75$ Deg., $\theta_s = 80$ Deg.,

$\Psi_t = 45$ Deg., $\Psi_s = 45$ Deg., $\phi_s = 0$ Deg.

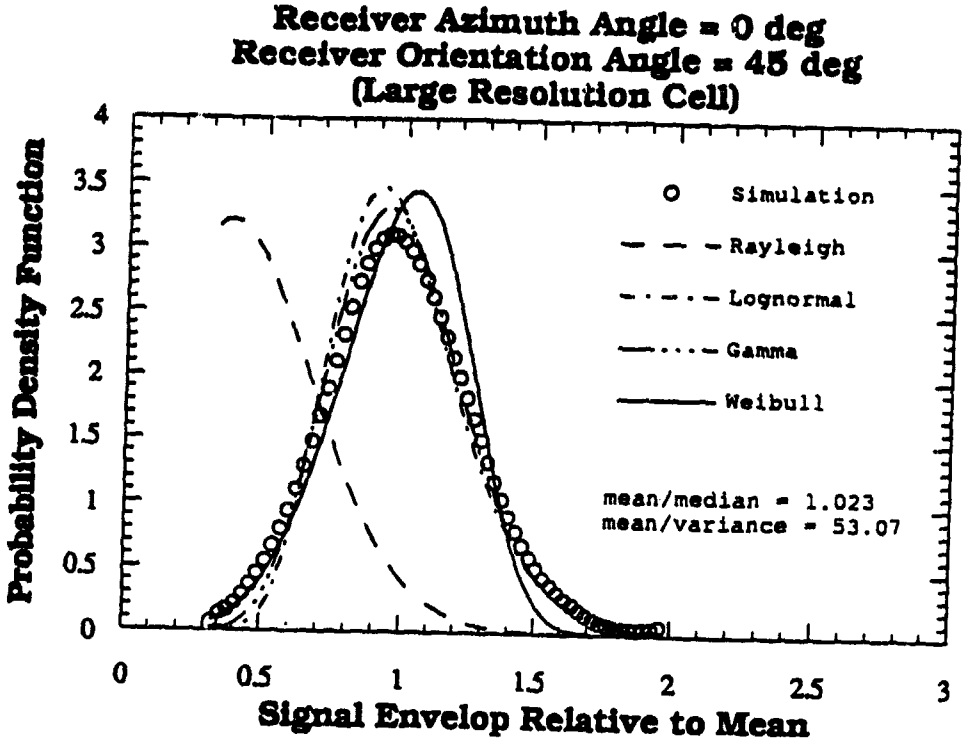

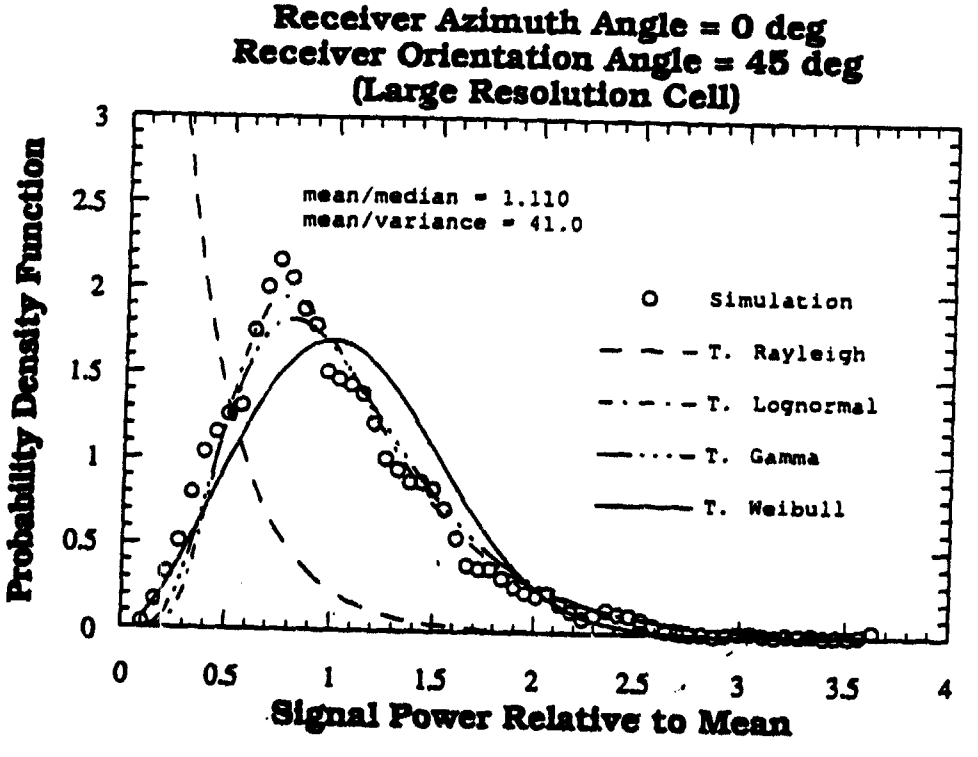

Figure 7c. Comparison between statistical models and simulated data for the large cell size.

Table 7c

Signal Envelope

Model	RMS Error	Model Parameters	
		shape	scale
Rayleigh	2.394		0.12
Lognormal	0.295	-1.20	0.25
Gamma	0.184	15.4	0.02
Weibull	0.118	4.81	0.34
mean= 3.1e-1		variance= 6.2e-3	

Signal Power

Model	RMS Error	Model Parameters	
		shape	scale
T. Rayleigh	3.854		0.12
T. Lognormal	0.616	-1.20	0.25
T. Gamma	0.643	15.4	0.02
T. Weibull	0.739	4.81	0.34
mean=1.0e-1		variance= 2.4e-3	

Large Resolution Cell

Cell Size = 12 Correlation Lengths

$\tau_t = \tau_s = 30$ Deg., $\theta_i = 75$ Deg., $\theta_s = 80$ Deg.,

$\Psi_t = 45$ Deg., $\Psi_s = 45$ Deg., $\phi_s = 0$ Deg.

Appendix A

I. Rough Surface Scattering Matrices

The bistatic single-scatter scattering coefficient matrix in the upper medium is given by

$$\bar{\sigma}^{\circ} = \frac{4\pi}{A}\langle \mathbf{S} \rangle \tag{A.1}$$

where A is the illuminated area and the elements of $\langle \mathbf{S} \rangle$ are equal to

$$\begin{bmatrix} \langle |S_{vv}|^2 \rangle & \langle |S_{vh}|^2 \rangle & Re\langle S_{vv} S_{vh}^* \rangle & -Im\langle S_{vv} S_{vh}^* \rangle \\ \langle |S_{hv}|^2 \rangle & \langle |S_{hh}|^2 \rangle & Re\langle S_{hv} S_{hh}^* \rangle & -Im\langle S_{hv} S_{hh}^* \rangle \\ 2Re\langle S_{vv} S_{hv}^* \rangle & 2Re\langle S_{vh} S_{vh}^* \rangle & Re\langle S_{vv} S_{hh}^* + S_{vh} S_{hv}^* \rangle & Im\langle S_{vh} S_{hv}^* - S_{vv} S_{hh}^* \rangle \\ 2Im\langle S_{vv} S_{hv}^* \rangle & 2Im\langle S_{vh} S_{hh}^* \rangle & Im\langle S_{vv} S_{hh}^* + S_{vh} S_{hv}^* \rangle & Re\langle S_{vv} S_{hh}^* - S_{vh} S_{hv}^* \rangle \end{bmatrix}$$

Each of the above matrix elements has the form.

$$\langle S_{qp} S_{rs}^* \rangle = \frac{k^2 A}{8\pi} exp\left[-\sigma^2 (k_z^2 + k_{sz}^2)\right] \sum_{n=1}^{\infty} \sigma^{2n} (I_{qp}^n I_{rs}^{n*}) \frac{W^{(n)}(k_{sx} - k_x, k_{sy} - k_y)}{n!} \tag{A.2}$$

where

$$I_{\alpha\beta}^n = (k_{sz} + k_z)^n f_{\alpha\beta} exp(-\sigma^2 k_z k_{sz}) + \frac{(k_{sz})^n F_{\alpha\beta}(-k_x, -k_y) + (k_z)^n F_{\alpha\beta}(-k_{sx}, -k_{sy})}{2} \tag{A.3}$$

In (A.3) the Kirchhoff field coefficients are given as

$$f_{vv} = \frac{2R_{\parallel}}{\cos\theta + \cos\theta_s}\left[\sin\theta \sin\theta_s - (1 + \cos\theta\cos\theta_s)\cos(\phi_s - \phi)\right] \tag{A.4}$$

$$f_{hh} = -\frac{2R_{\perp}}{\cos\theta + \cos\theta_s}\left[\sin\theta \sin\theta_s - (1 + \cos\theta\cos\theta_s)\cos(\phi_s - \phi)\right] \tag{A.5}$$

$$f_{hv} = 2R\sin(\phi_s - \phi) \tag{A.6}$$

$$f_{vh} = 2R\sin(\phi - \phi_s) \tag{A.7}$$

where $R = (R_{\parallel} - R_{\perp})/2$. For simplicity of writing we shall use the following notations

in writing the complementary field coefficients.

$$s = \sin\theta, ss = \sin\theta_s$$

$$cs = \cos\theta, css = \cos\theta_s, sf = \sin(\phi_s - \phi), csf = \cos(\phi_s - \phi)$$

$$sq = (\mu_r\varepsilon_r - \sin^2\theta)^{1/2}, sqs = (\mu_r\varepsilon_r - \sin^2\theta_s)^{1/2}$$

$$r = (sqcss)/(sqscs)$$

$$\mu_r = \mu_t/\mu, \varepsilon_r = \varepsilon_t/\varepsilon$$

$$c1 = (csf - sss)/(sqcss)$$

$$c1s = (csf - sss)/(sqscs)$$

$$c2 = s(ss - scsf)/css$$

$$c2s = s(ss - sscsf)/cs$$

$$T_v = 1 + R_{\parallel}, T_{vm} = 1 - R_{xx}$$

$$T_h = 1 + R_{\perp}, T_{hm} = 1 - R_{\perp}$$

$$T_p = 1 + R, T_m = 1 - R$$

Using the above notations we can write the complementary field coefficients as

$$F_{vv}(-k_x, -k_y) = -(csT_{vm} - sqT_v/\varepsilon_r)(T_v csf + T_{vm}\varepsilon_r c1) + (T_{vm}^2 - csT_vT_{vm}/sq)c2 \quad \text{(A.8)}$$

$$F_{hh}(-k_x, -k_y) = (csT_{hm} - sqT_h/\mu_r)(T_h csf + T_{hm}\mu_r c1) - (ch - csT_hT_{hm}/sq)c2 \quad \text{(A.9)}$$

$$F_{hv}(-k_x, -k_y) = (csT_m - sqT_p/\varepsilon_r)(T_p/css + T_m\varepsilon_r/sq)sf + (cvh - csT_pT_m/sq)s^2 sf \quad \text{(A.10)}$$

$$F_{vh}(-k_x, -k_y) = (csT_p - sqT_m/\mu_r)(T_m/css + T_p\mu_r/sq)sf + (cvh - csT_pT_m/sq)s^2 sf \quad \text{(A.11)}$$

$$F_{vv}(-k_{xs}, -k_{sy}) = -(cssT_{vm} - sqsT_v/\varepsilon_r)(T_v csf + T_{vm}\varepsilon_r c1s) + (cv - cssT_vT_{vm}/sqs)c2s \quad \text{(A.12)}$$

$$F_{hh}(-k_{xs}, -k_{sy}) = (cssT_{hm} - sqsT_h/\mu_r)(T_h csf + T_{hm}\mu_r c1s) - (ch - cssT_hT_{hm}/sqs)c2s \quad \text{(A.13)}$$

$$F_{hv}(-k_{sx}, -k_{sy}) = -(cssT_p - sqsT_m/\mu_r)(T_m/cs + T_p\mu_r/sqs)sf$$

$$-(cvh - cssT_pT_m/sqs)\,ss^2sf \tag{A.14}$$

$$F_{vh}(-k_{sx}, -k_{sy}) = -(cssT_m - sqsT_p/\varepsilon_r)\,(T_p/cs + T_m\varepsilon_r/sqs)\,sf$$
$$-(cvh - cssT_pT_m/sqs)\,ss^2sf \tag{A.15}$$

$$R_{\parallel} = \frac{\varepsilon_r cs - sq}{\varepsilon_r cs + sq} \tag{A.16}$$

$$R_{\perp} = \frac{\mu_r cs - sq}{\mu_r cs + sq} \tag{A.17}$$

$$R_r = (1 - R)/(1 + R) \tag{A.18}$$

$$k_x = k\sin\theta\cos\phi;\; k_y = k\sin\theta\sin\phi;\; k_z = k\cos\theta \tag{A.19}$$

$$k_{sx} = k\sin\theta_s\cos\phi_s;\; k_{sy} = k\sin\theta_s\sin\phi_s;\; k_{sz} = k\cos\theta_s \tag{A.20}$$

Appendix B

This appendix summarizes all the cases included in previous reports. The first thirty cases are for cross polarization with receiver orientation angle along 135 degrees while the incident angle of orientation is along 45 degrees. The 30 cases include to 5 azimuthal angles, 3 cell sizes and displays in terms of signal amplitude and power. These are denoted as Figures B1 through B 5 Then, there are 12 cases for polarized scattering with receiver orientation angle along 45 degrees and azimuthal angle chosen to be 180 and 135 degrees. These are denoted as Figures B6 through B7. Each figure shows both amplitude distribution and power distribution for a given set of angles followed by a table showing rms error calculations for the different distribution functions shown in the figure. The set of angles for a given case is marked on the figures and given below the tables.

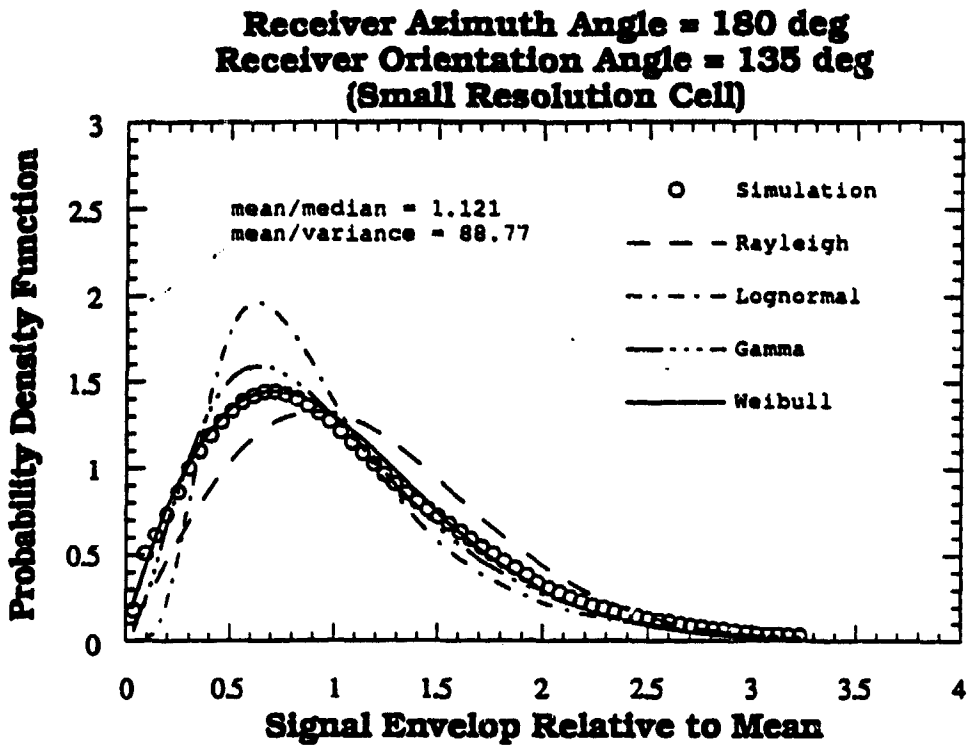

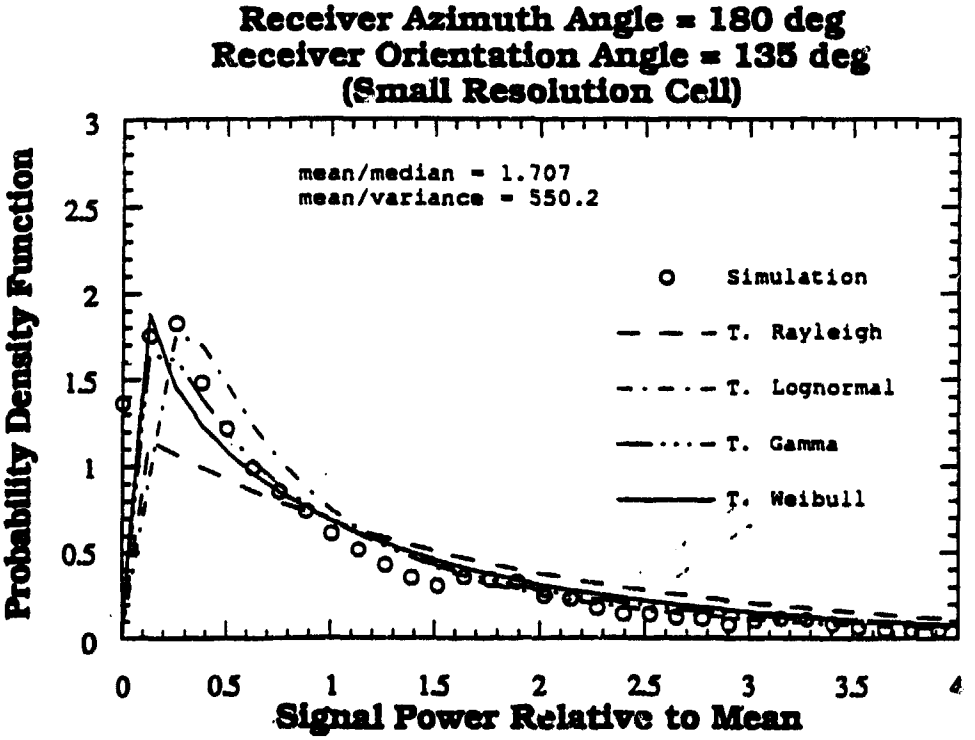

Figure B1a. Comparison between statistical models and simulated data for the small cell size.

Table 1a

Signal Envelope

Model	RMS Error	Model Parameters	
		shape	scale
Rayleigh	2.534		0.029
Lognormal	2.338	-3.6	0.55
Gamma	1.022	2.81	0.011
Weibull	0.659	1.8	0.036
mean= 3.0e-2		variance= 4.0e-4	

Signal Power

Model	RMS Error	Model Parameters	
		shape	scale
T. Rayleigh	30.33		0.029
T. Lognormal	22.62	-3.6	0.55
T. Gamma	18.95	2.81	0.011
T. Weibull	17.99	1.8	0.036
mean= 1.3e-3		variance= 2.0e-6	

Small Resolution Cell

Cell Size = 4 Correlation Lengths

$\tau_t = \tau_s = 30$ Deg., $\theta_i = 75$ Deg., $\theta_s = 80$ Deg.,

$\psi_t = 45$ Deg., $\psi_s = 135$ Deg., $\phi_s = 180$ Deg.

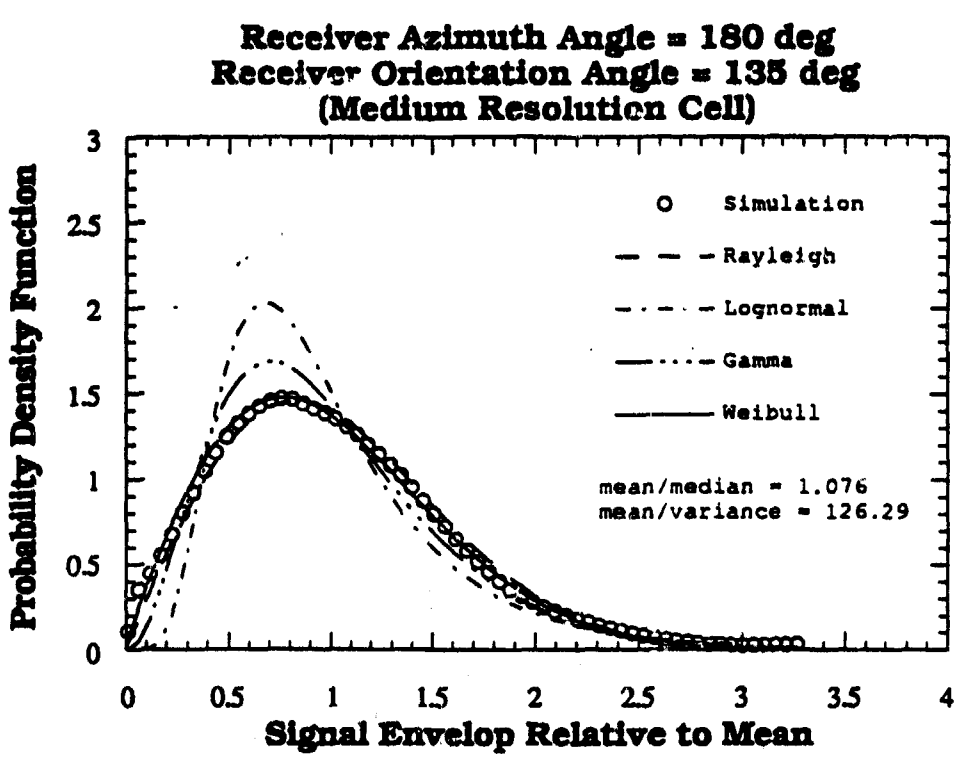

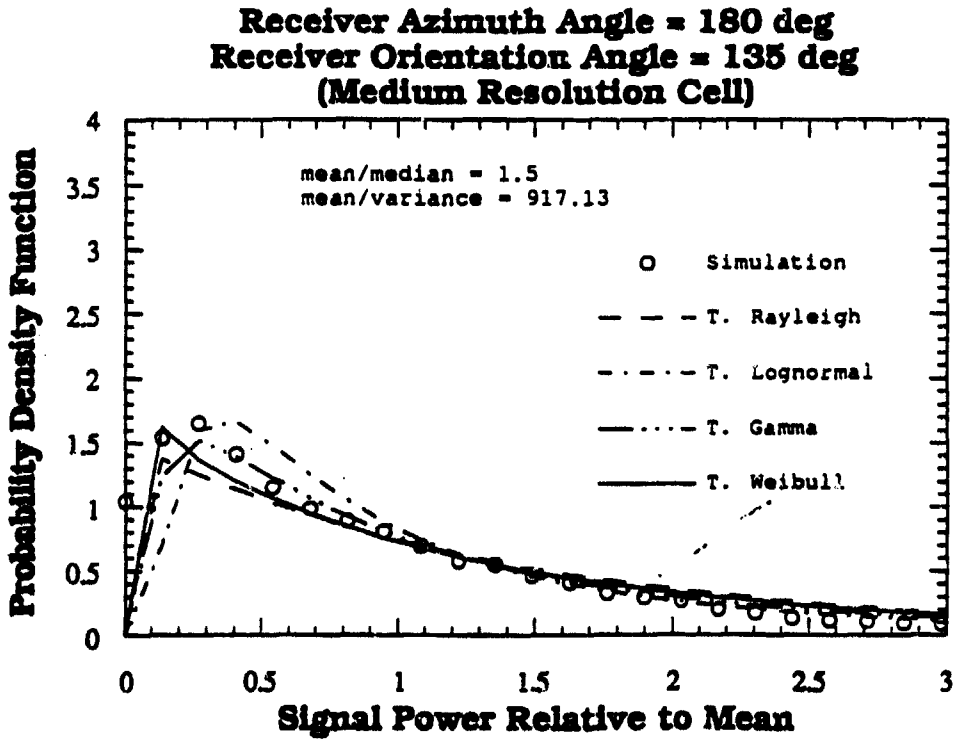

Figure B1b. Comparison between statistical models and simulated data for the medium cell size.

Table 1b

Signal Envelope

Model	RMS Error	Model Parameters	
		shape	scale
Rayleigh	0.952		0.022
Lognormal	2.887	-3.75	0.511
Gamma	1.320	3.35	0.008
Weibull	0.824	1.87	0.03
mean= 2.7e-2		variance= 2.1e-4	

Signal Power

Model	RMS Error	Model Parameters	
		shape	scale
T. Rayleigh	24.66		0.022
T. Lognormal	31.52	-3.75	0.511
T. Gamma	22.33	3.35	0.008
T. Weibull	18.59	1.87	0.03
mean= 9.2e-4		variance= 1.2e-6	

Medium Resolution Cell

Cell Size = 8 Correlation Lengths

$\tau_t = \tau_s = 30$ Deg., $\theta_i = 75$ Deg., $\theta_s = 80$ Deg.,

$\Psi_t = 45$ Deg, $\Psi_s = 135$ Deg., $\phi_s = 180$ Deg.

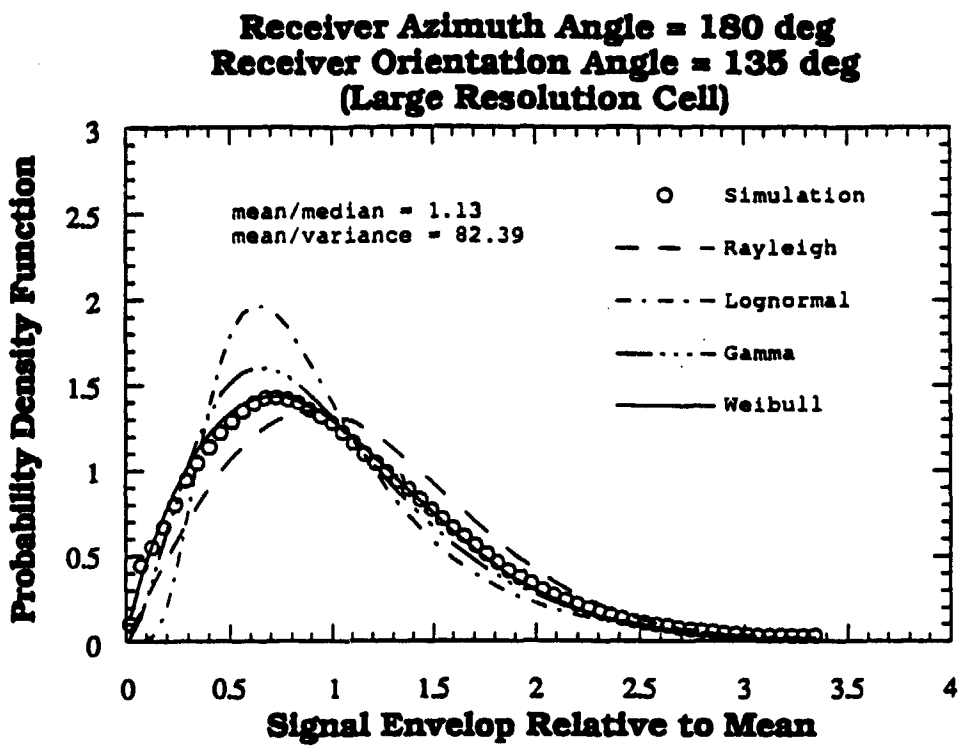

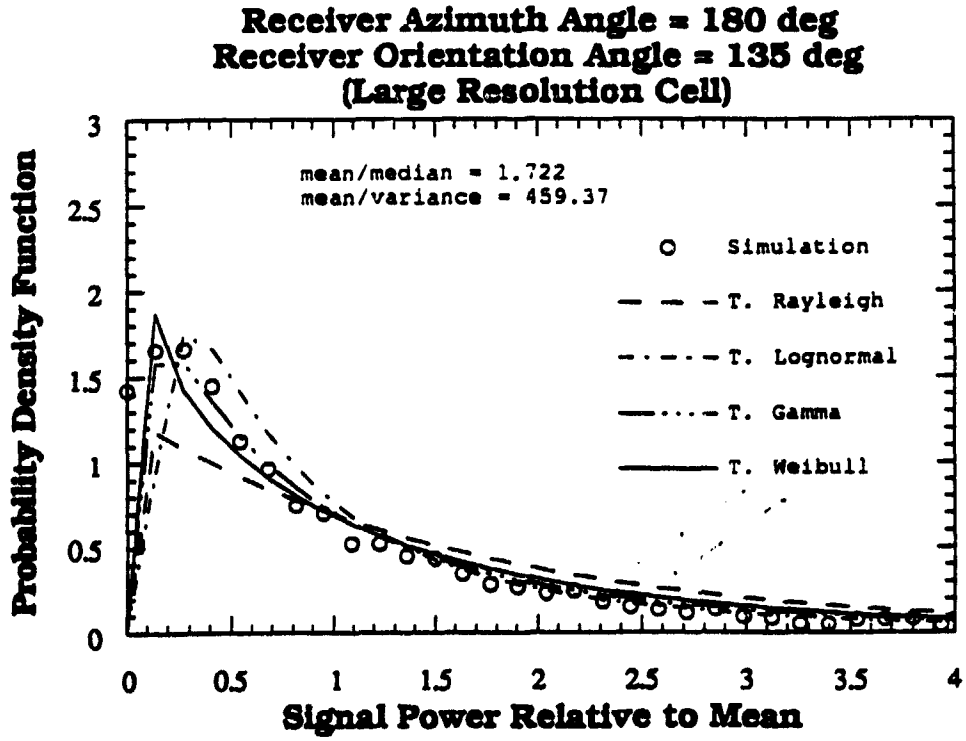

Figure B1c. Comparison between statistical models and simulated data for the large cell size.

Table 1c

Signal Envelope

Model	RMS Error	Model Parameters	
		shape	scale
Rayleigh	1.669		0.032
Lognormal	2.158	-3.49	0.54
Gamma	0.654	2.9	0.012
Weibull	0.299	1.79	0.04
mean= 3.5e-2		variance= 4.2e-4	

Signal Power

Model	RMS Error	Model Parameters	
		shape	scale
T. Rayleigh	20.23		0.032
T. Lognormal	19.32	-3.49	0.54
T. Gamma	12.74	2.9	0.012
T. Weibull	11.26	1.79	0.04
mean= 1.6e-3		variance= 3.6e-6	

Large Resolution Cell

Cell Size = 12 Correlation Lengths

$\tau_t = \tau_s = 30$ Deg., $\theta_i = 75$ Deg., $\theta_s = 80$ Deg.,

$\psi_t = 45$ Deg., $\psi_s = 135$ Deg., $\phi_s = 180$ Deg.

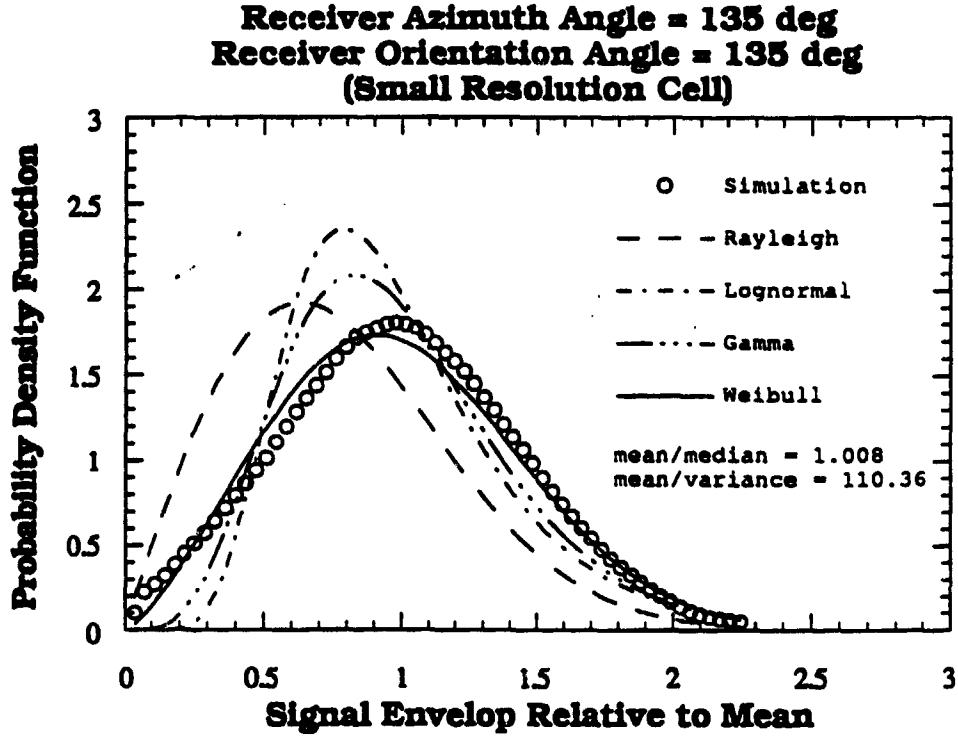

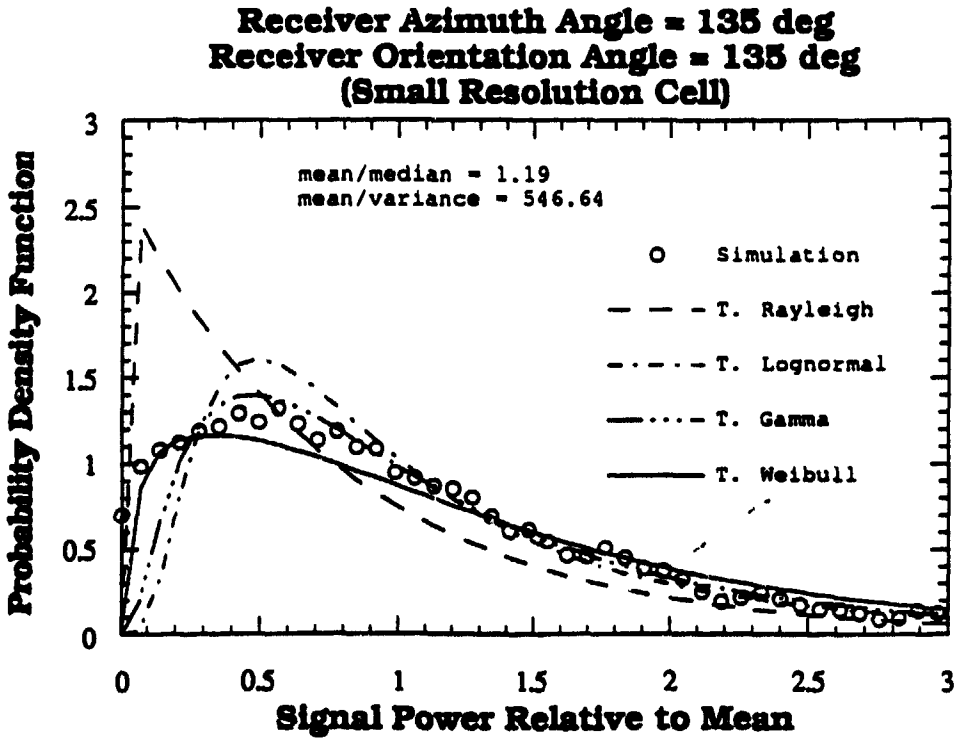

Figure B2a. Comparison between statistical models and simulated data for the small cell size.

Table 2a

Signal Envelope

Model	RMS Error	Model Parameters	
		shape	scale
Rayleigh	3.412		0.034
Lognormal	2.351	-3.02	0.41
Gamma	1.498	5.67	0.009
Weibull	0.901	2.35	0.06
mean= 5.3e-2		variance= 5.0e-4	

Signal Power

Model	RMS Error	Model Parameters	
		shape	scale
T. Rayleigh	34.55		0.034
T. Lognormal	28.64	-3.02	0.41
T. Gamma	30.28	5.67	0.009
T. Weibull	19.22	2.35	0.06
mean= 3.3e-3		variance= 6.3e-6	

Small Resolution Cell

Cell Size = 4 Correlation Lengths

$\tau_t = \tau_s = 30$ Deg., $\theta_i = 75$ Deg., $\theta_s = 80$ Deg.,

$\Psi_t = 45$ Deg., $\Psi_s = 135$ Deg., $\phi_s = 135$ Deg.

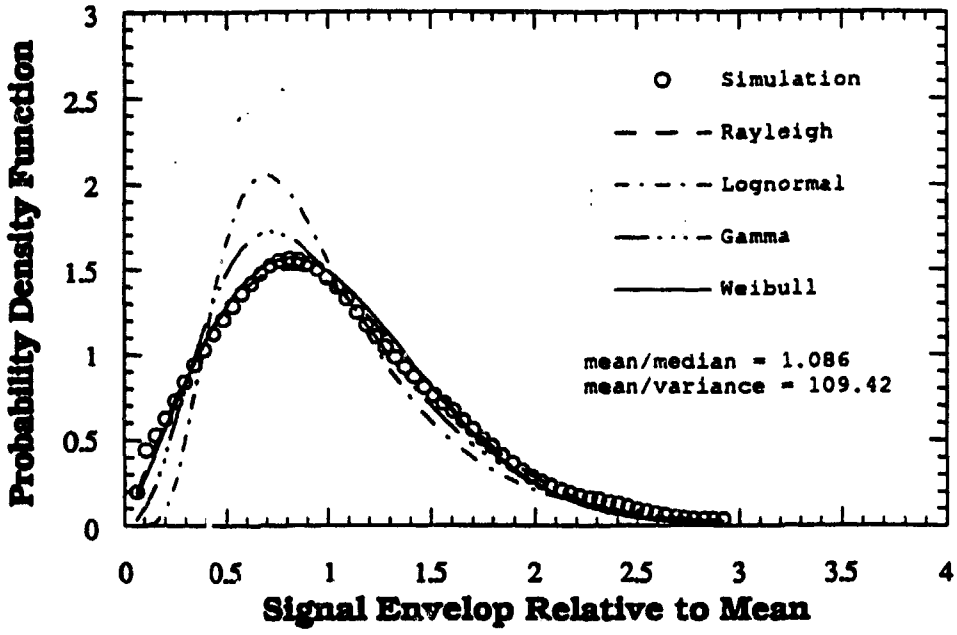

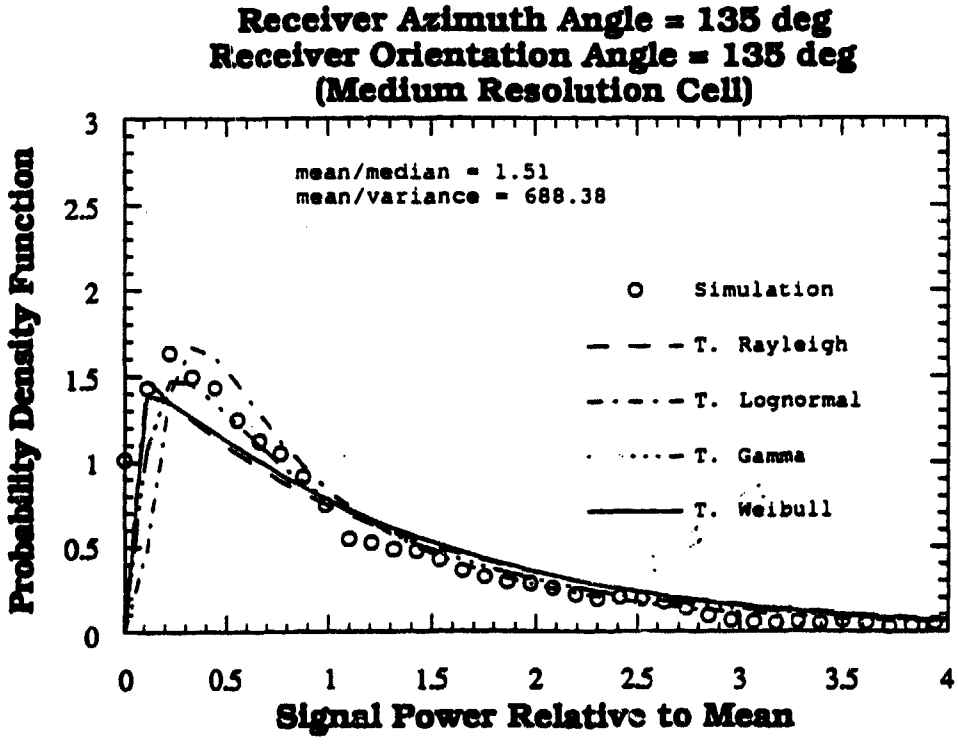

Figure B2b. Comparison between statistical models and simulated data for the medium cell size.

Table 2b

Signal Envelope

Model	RMS Error	Model Parameters	
		shape	scale
Rayleigh	0.806		0.27
Lognormal	2.511	-3.54	0.5
Gamma	1.094	3.55	0.009
Weibull	0.652	2.02	0.037
mean= 3.3e-2		variance= 3.0e-4	

Signal Power

Model	RMS Error	Model Parameters	
		shape	scale
T. Rayleigh	22.39		0.27
T. Lognormal	31.09	-3.54	0.5
T. Gamma	45.32	3.55	0.009
T. Weibull	20.37	2.02	0.037
mean= 1.4e-3		variance= 2.0e-6	

Medium Resolution Cell

Cell Size = 8 Correlation Lengths

$\tau_t = \tau_s = 30$ Deg., $\theta_i = 75$ Deg., $\theta_s = 80$ Deg.,

$\psi_t = 45$ Deg., $\psi_s = 135$ Deg., $\phi_s = 135$ Deg.

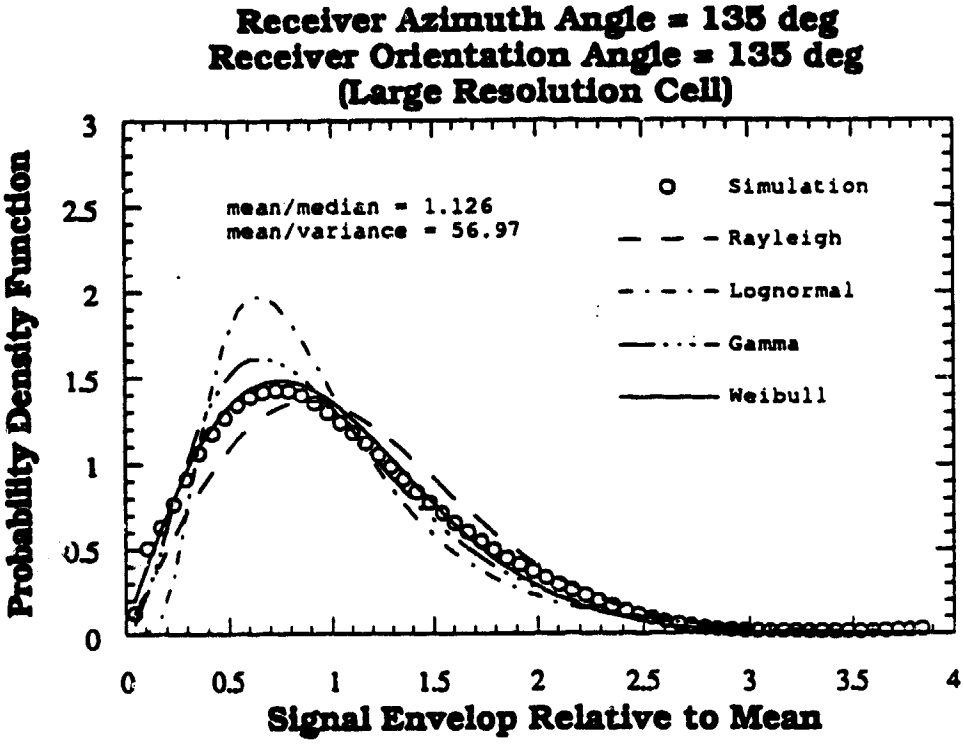

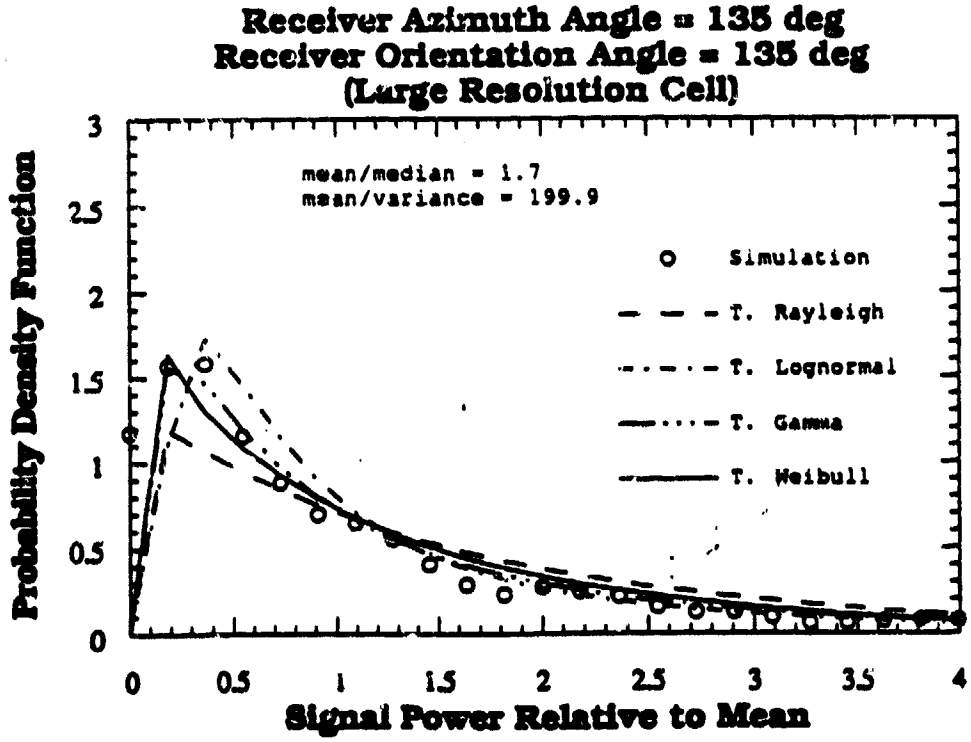

Figure B2c. Comparison between statistical models and simulated data for the large cell size.

Table 2c

Signal Envelope

Model	RMS Error	Model Parameters	
		shape	scale
Rayleigh	1.138		0.047
Lognormal	1.451	-3.09	0.54
Gamma	0.508	2.97	0.018
Weibull	0.377	1.90	0.059
mean= 5.3e-2		variance= 9.0e-4	

Signal Power

Model	RMS Error	Model Parameters	
		shape	scale
T. Rayleigh	6.784		0.047
T. Lognormal	5.663	-3.09	0.54
T. Gamma	7.521	2.97	0.018
T. Weibull	4.398	1.90	0.059
mean= 3.6e-3		variance= 1.8e-5	

Large Resolution Cell

Cell Size = 12 Correlation Lengths

$\tau_t = \tau_s = 30$ Deg., $\theta_i = 75$ Deg., $\theta_s = 80$ Deg.,

$\Psi_t = 45$ Deg., $\Psi_s = 135$ Deg., $\phi_s = 135$ Deg.

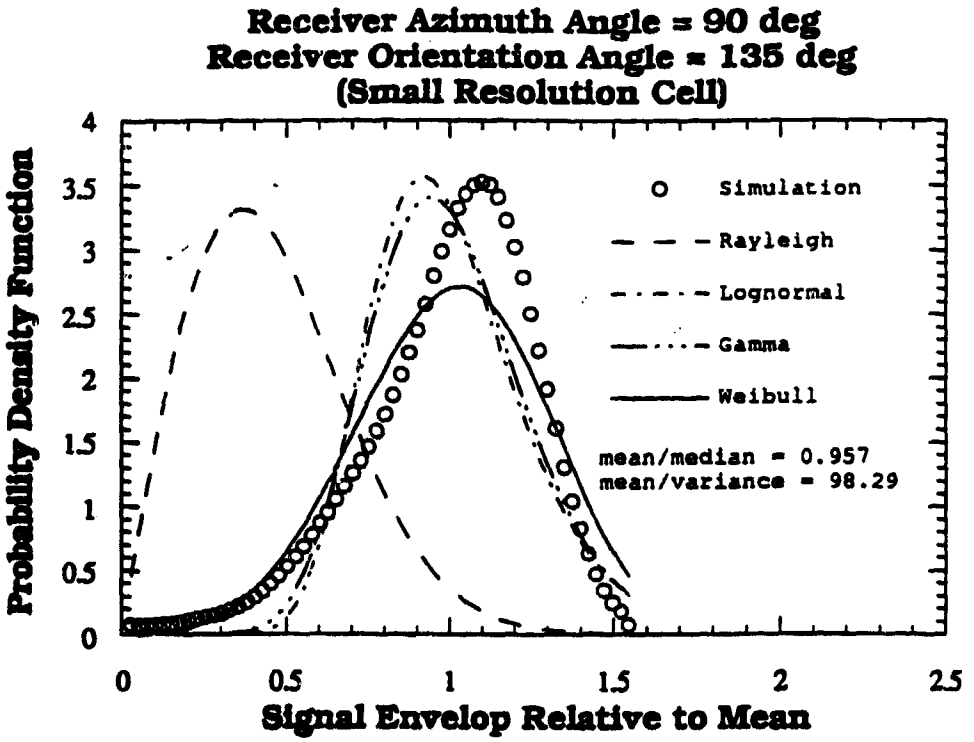

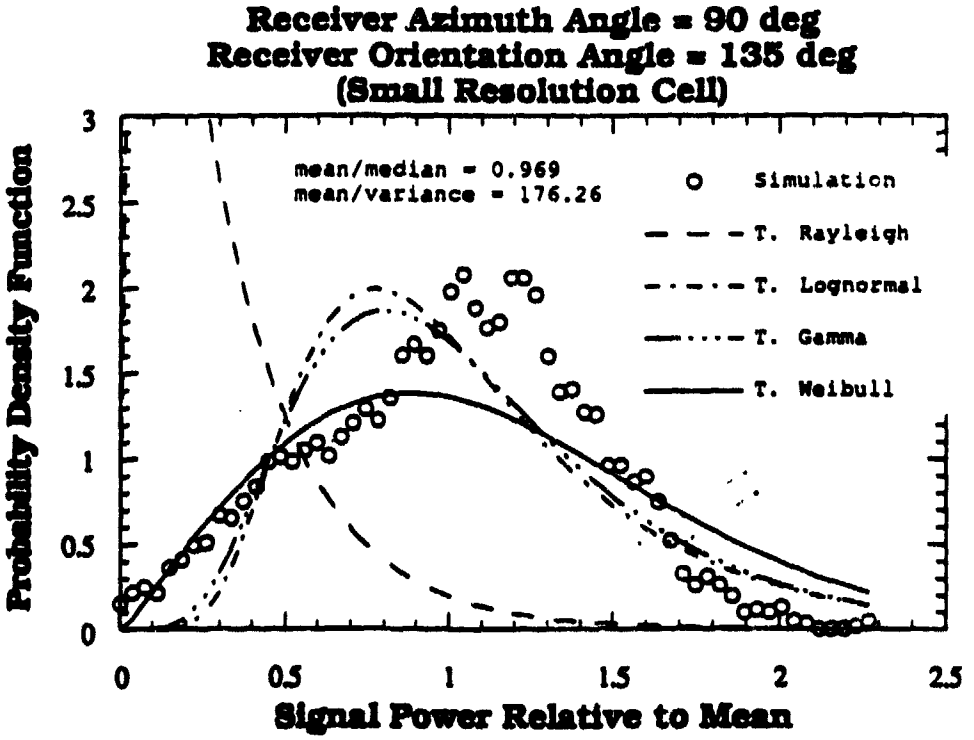

Figure B3a. Comparison between statistical models and simulated data for the small cell size.

Table 3a

Signal Envelope

Model	RMS Error	Model Parameters	
		shape	scale
Rayleigh	5.672		0.019
Lognormal	1.573	-1.76	0.24
Gamma	1.354	16.5	0.011
Weibull	1.120	3.79	0.20
mean= 1.8e-1		variance= 1.9e-3	

Signal Power

Model	RMS Error	Model Parameters	
		shape	scale
T. Rayleigh	18.62		0.019
T. Lognormal	7.984	-1.76	0.24
T. Gamma	6.995	16.5	0.011
T. Weibull	6.310	3.79	0.20
mean= 3.3e-2		variance= 2.0e-4	

Small Resolution Cell

Cell Size = 4 Correlation Lengths

$\tau_t = \tau_s = 30$ Deg., $\theta_i = 75$ Deg., $\theta_s = 80$ Deg.,

$\Psi_t = 45$ Deg., $\Psi_s = 135$ Deg., $\phi_s = 90$ Deg.

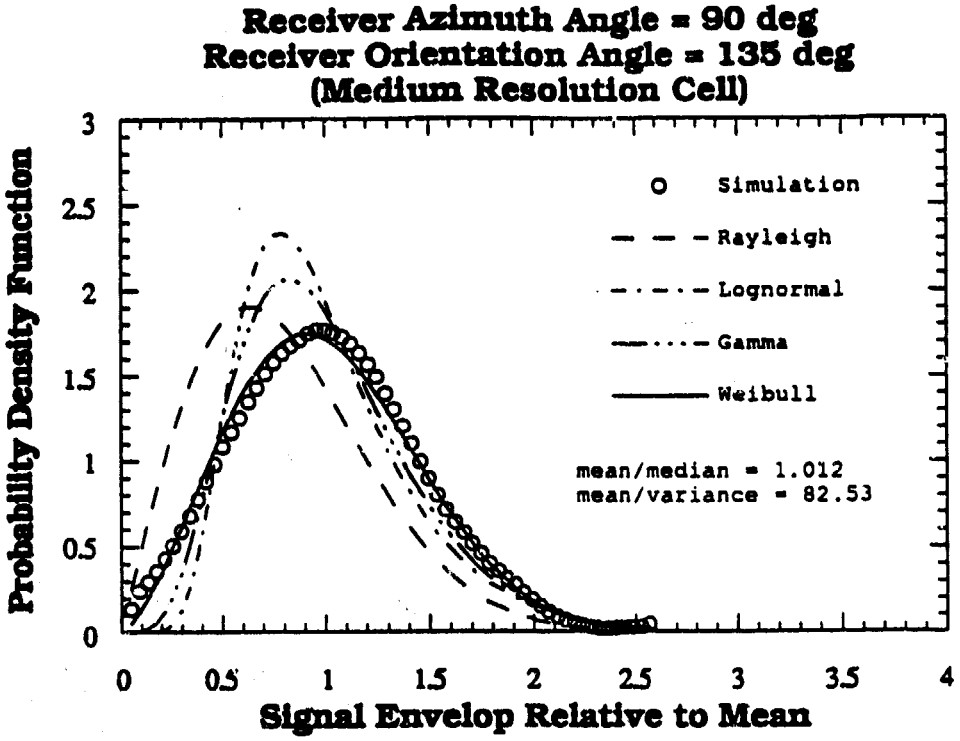

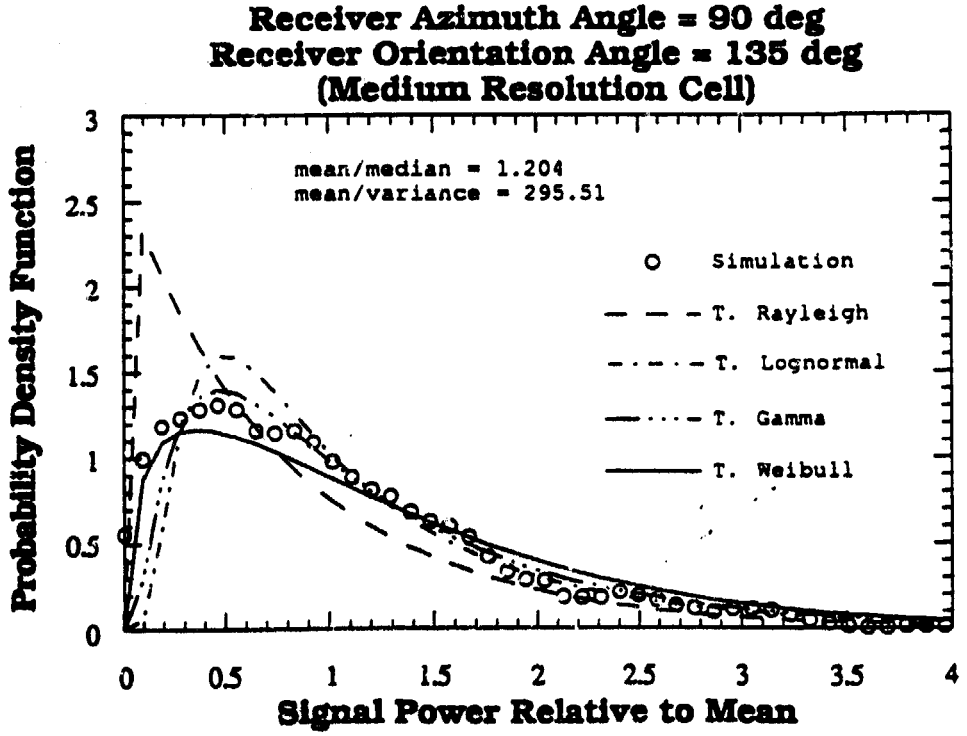

Figure B3b. Comparison between statistical models and simulated data for the medium cell size.

Table 3b

Signal Envelope

Model	RMS Error	Model Parameters	
		shape	scale
Rayleigh	2.331		0.05
Lognormal	1.794	-2.75	0.41
Gamma	1.120	5.56	0.013
Weibull	0.514	2.4	0.079
mean= 7.0e-2		variance= 9.0e-4	

Signal Power

Model	RMS Error	Model Parameters	
		shape	scale
T. Rayleigh	13.79		0.05
T. Lognormal	11.20	-2.75	0.41
T. Gamma	8.631	5.56	0.013
T. Weibull	7.568	2.4	0.079
mean= 5.6e-3		variance= 2.0e-5	

Medium Resolution Cell

Cell Size = 8 Correlation Lengths

$\tau_t = \tau_s = 30$ Deg., $\theta_i = 75$ Deg., $\theta_s = 30$ Deg.,

$\psi_t = 45$ Deg., $\psi_s = 135$ Deg., $\phi_s = 90$ Deg.

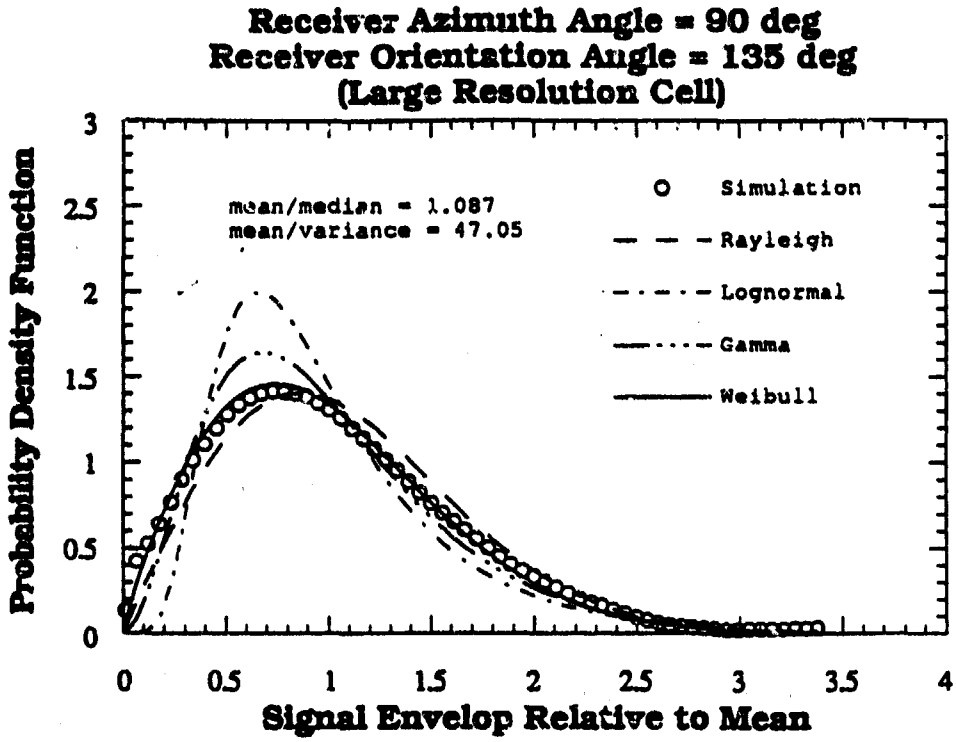

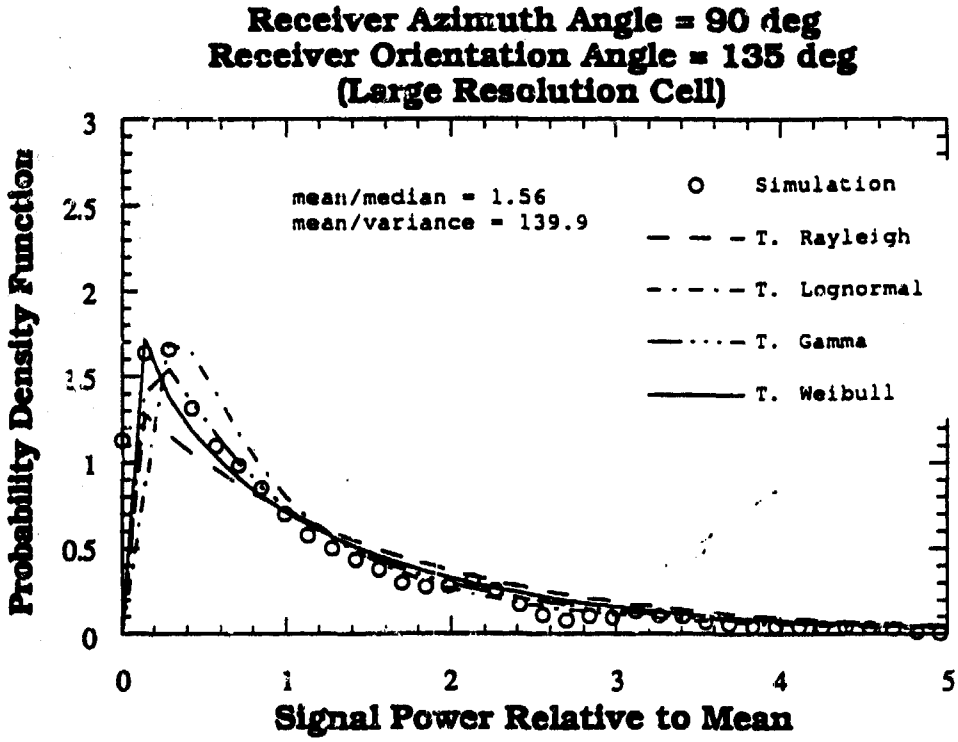

Figure B3c. Comparison between statistical models and simulated data for the large cell size.

Table 3c

Signal Envelope

Model	RMS Error	Model Parameters	
		shape	scale
Rayleigh	0.506		0.058
Lognormal	1.285	-2.85	0.53
Gamma	0.540	3.08	0.022
Weibull	0.189	1.78	0.075
mean= 6.7e-2		variance= 1.5e-3	

Signal Power

Model	RMS Error	Model Parameters	
		shape	scale
T. Rayleigh	4.978		0.058
T. Lognormal	5.211	-2.85	0.53
T. Gamma	3.988	3.08	0.022
T. Weibull	2.016	1.78	0.075
mean= 5.8e-3		variance= 4.2e-5	

Large Resolution Cell

Cell Size = 12 Correlation Lengths

$\tau_t = \tau_s = 30$ Deg., $\theta_i = 75$ Deg., $\theta_s = 80$ Deg.,

$\Psi_t = 45$ Deg., $\Psi_s = 135$ Deg., $\phi_s = 90$ Deg.

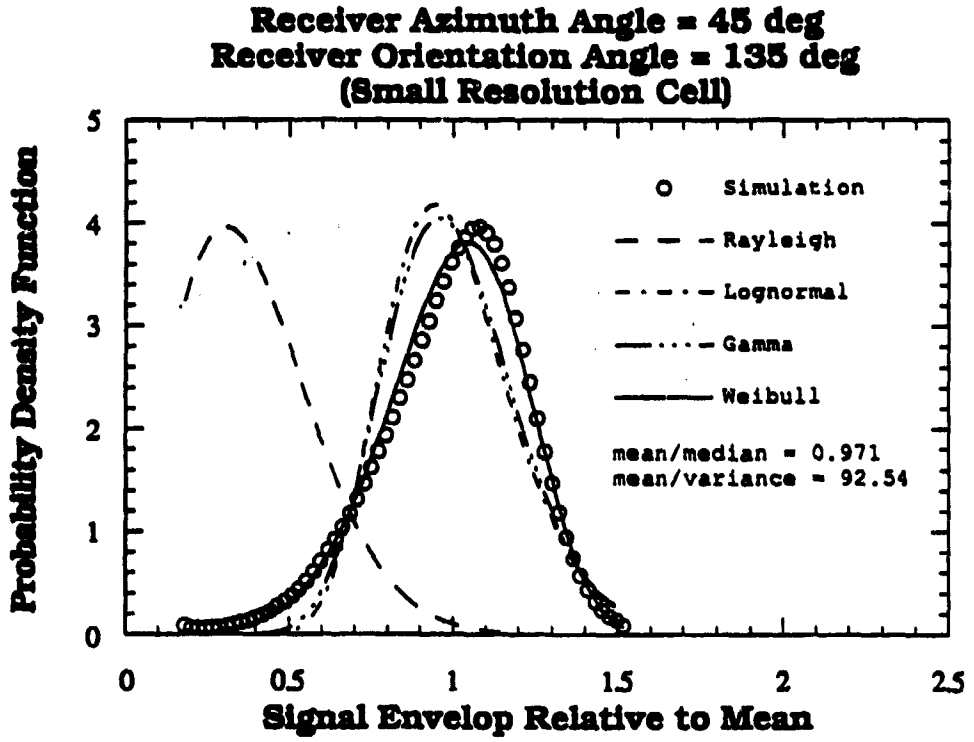

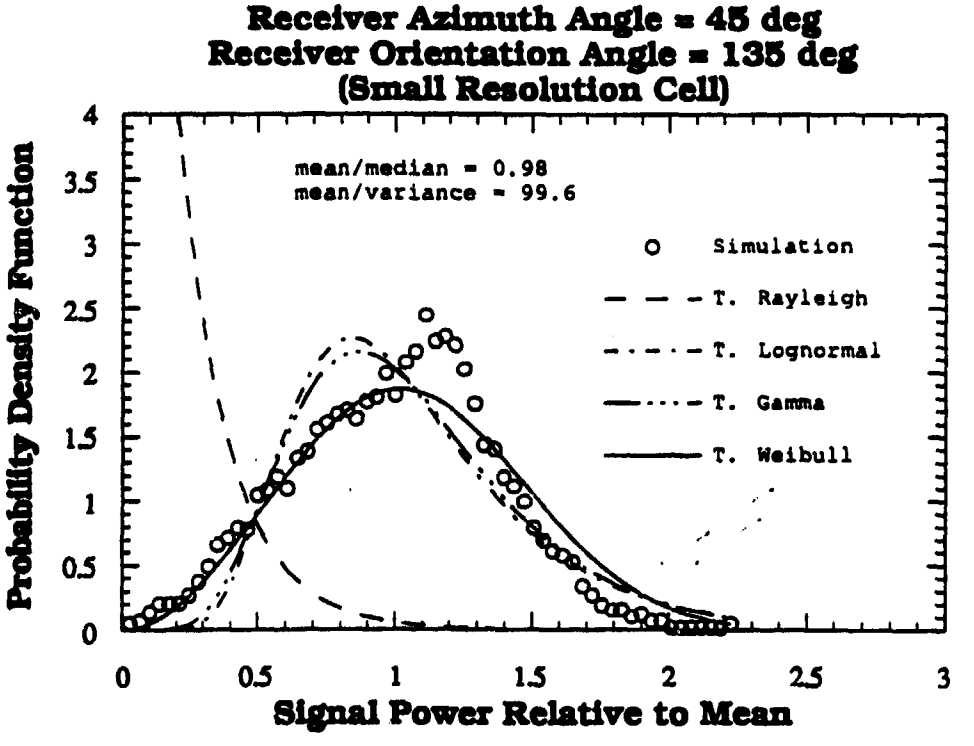

Figure B4a. Comparison between statistical models and simulated data for the small cell size.

Table 4a

Signal Envelope

Model	RMS Error	Model Parameters	
		shape	scale
Rayleigh	4.197		0.09
Lognormal	1.025	-1.33	0.20
Gamma	0.811	23.4	0.012
Weibull	0.408	5.30	0.29
mean= 2.7e-1		variance= 3.0e-3	

Signal Power

Model	RMS Error	Model Parameters	
		shape	scale
T. Rayleigh	9.368		0.09
T. Lognormal	2.991	-1.33	0.20
T. Gamma	2.854	23.4	0.012
T. Weibull	1.998	5.30	0.29
mean= 7.6e-2		variance= 7.6e-4	

Small Resolution Cell

Cell Size = 4 Correlation Lengths

$\tau_t = \tau_s = 30$ Deg., $\theta_i = 75$ Deg., $\theta_s = 80$ Deg.,

$\psi_t = 45$ Deg., $\psi_s = 135$ Deg., $\phi_s = 45$ Deg.

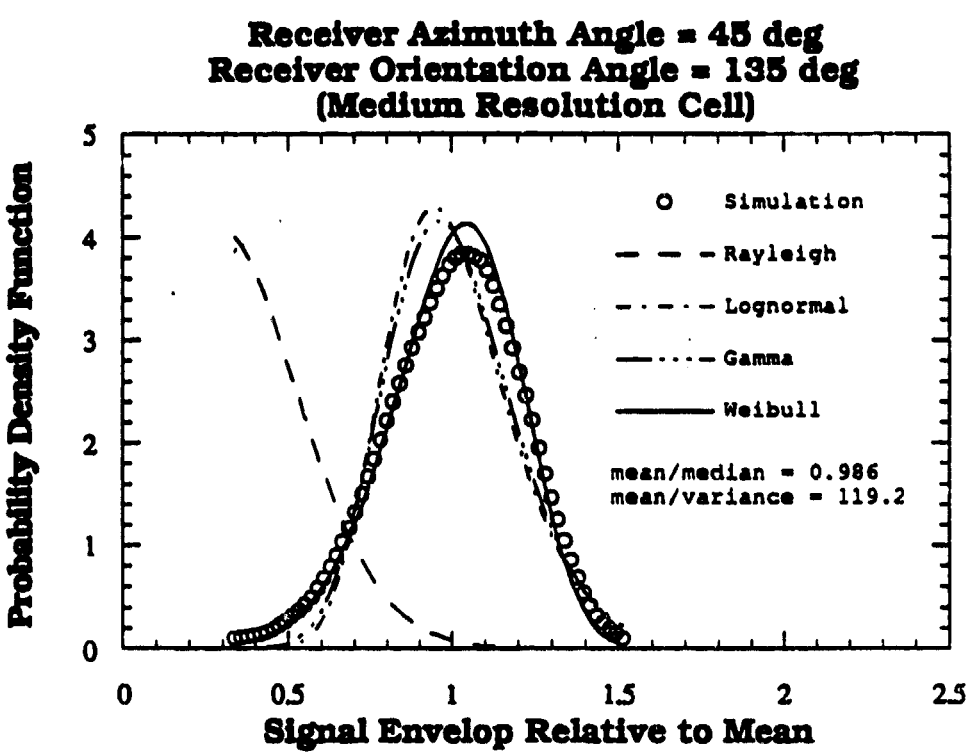

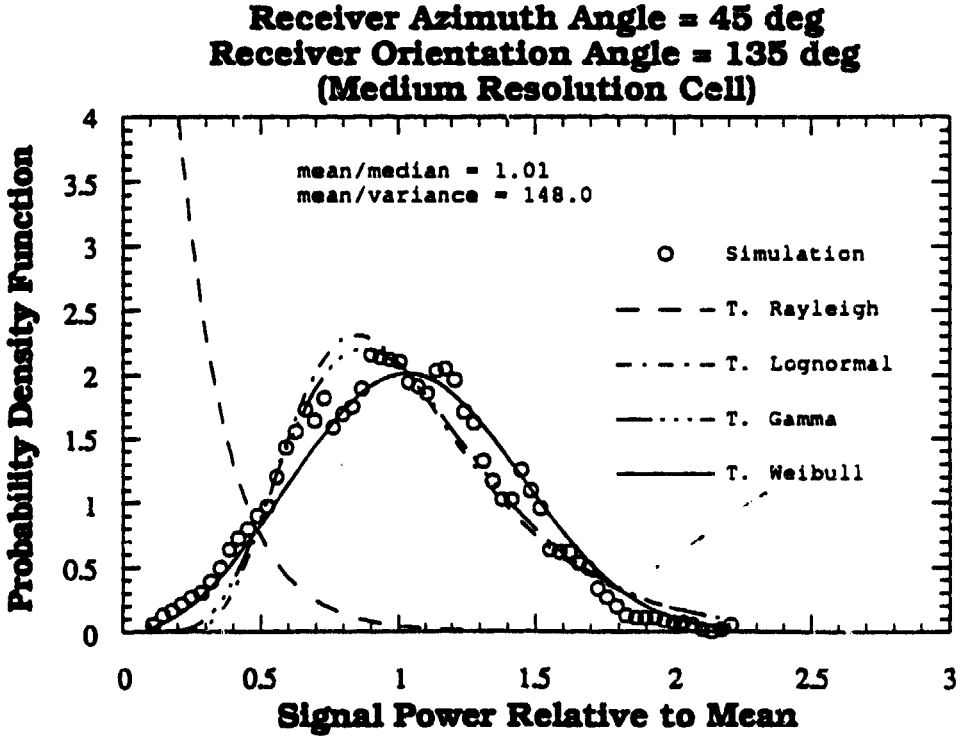

Figure B4b. Comparison between statistical models and simulated data for the medium cell size.

Table 4b

Signal Envelope

Model	RMS Error	Model Parameters	
		shape	scale
Rayleigh	5.214		0.067
Lognormal	1.057	-1.53	0.20
Gamma	0.821	25.2	0.009
Weibull	0.097	5.85	0.24
mean= 2.2e-1		variance= 2.0e-3	

Signal Power

Model	RMS Error	Model Parameters	
		shape	scale
T. Rayleigh	11.25		0.067
T. Lognormal	4.221	-1.53	0.20
T. Gamma	4.057	25.2	0.009
T. Weibull	2.552	5.85	0.24
mean=5.1e-2		variance= 3.5e-4	

Medium Resolution Cell

Cell Size = 8 Correlation Lengths

$\tau_t = \tau_s = 30$ Deg., $\theta_i = 75$ Deg., $\theta_s = 80$ Deg.,

$\Psi_t = 45$ Deg., $\Psi_s = 135$ Deg., $\phi_s = 45$ Deg.

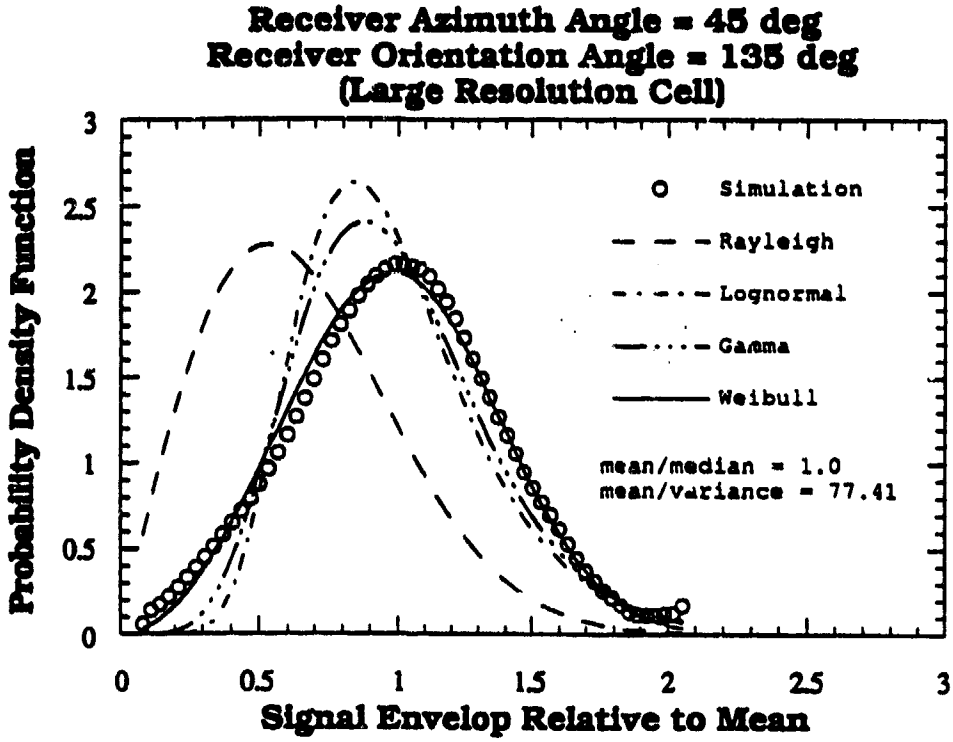

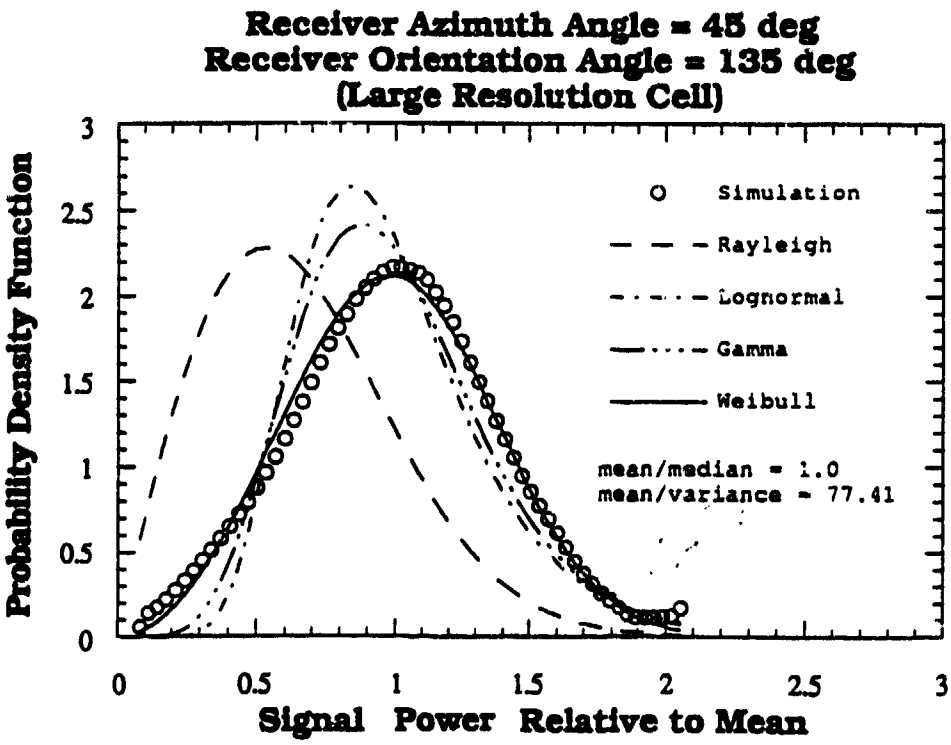

Figure B4c. Comparison between statistical models and simulated data for the large cell size.

Table 4c

Signal Envelope

Model	RMS Error	Model Parameters	
		shape	scale
Rayleigh	3.584		0.06
Lognormal	1.517	-2.30	0.35
Gamma	1.025	7.89	0.013
Weibull	0.497	2.96	0.12
mean= 1.1e-1		variance= 1.4e-3	

Signal Power

Model	RMS Error	Model Parameters	
		shape	scale
T. Rayleigh	17.18		0.06
T. Lognormal	8.612	-2.30	0.35
T. Gamma	7.968	7.89	0.013
T. Weibull	5.654	2.96	0.12
mean= 1.3e-2		variance= 7.0e-5	

Large Resolution Cell

Cell Size = 12 Correlation Lengths

$\tau_t = \tau_s = 30$ Deg., $\theta_i = 75$ Deg., $\theta_s = 80$ Deg.,

$\psi_t = 45$ Deg., $\psi_s = 135$ Deg., $\phi_s = 45$ Deg.

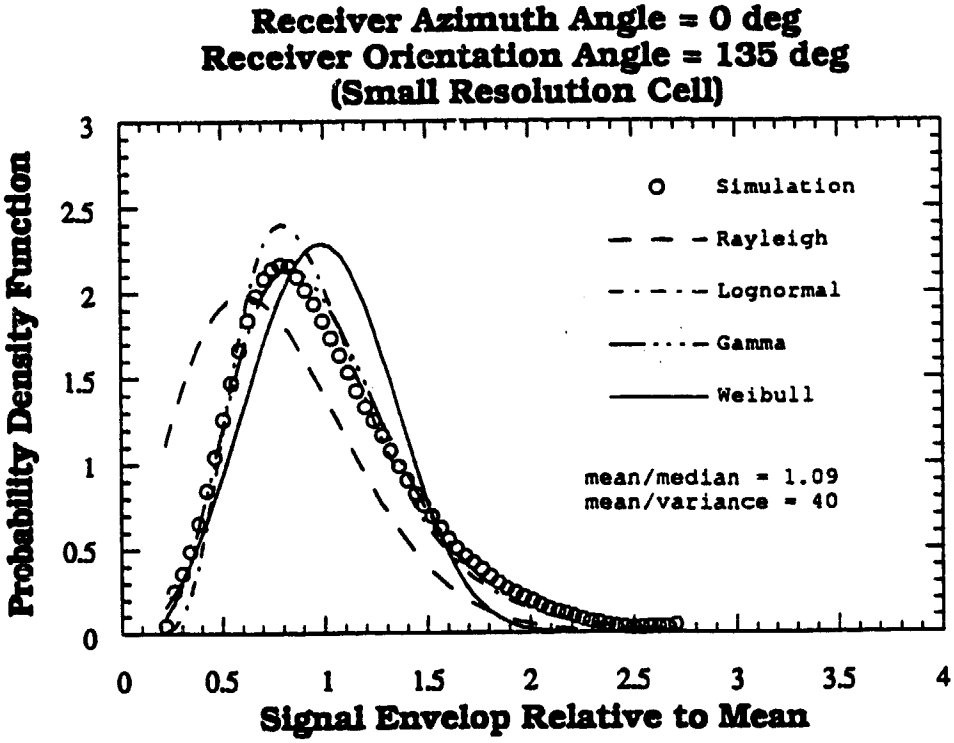

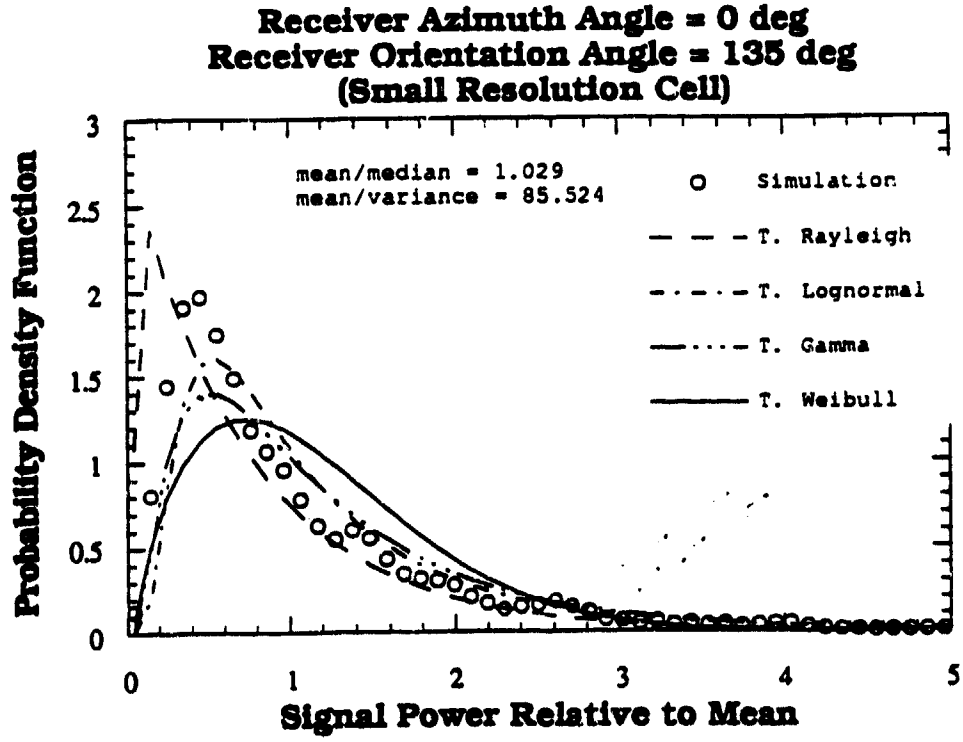

Figure B5a. Comparison between statistical models and simulated data for the small cell size.

Table 5a

Signal Envelope

Model	RMS Error	Model Parameters	
		shape	scale
Rayleigh	1.022		0.10
Lognormal	1.108	-1.93	0.39
Gamma	1.091	6.03	0.026
Weibull	1.228	3.17	0.17
mean= 1.1e-1		variance= 1.4e-3	

Signal Power

Model	RMS Error	Model Parameters	
		shape	scale
T. Rayleigh	2.345		0.10
T. Lognormal	1.318	-1.93	0.39
T. Gamma	1.201	6.03	0.026
T. Weibull	1.561	3.17	0.17
mean= 2.8e-2		variance= 6.0e-4	

Small Resolution Cell

Cell Size = 4 Correlation Lengths

$\tau_t = \tau_s = 30$ Deg., $\theta_i = 75$ Deg., $\theta_s = 80$ Deg.,

$\Psi_t = 45$ Deg., $\Psi_s = 135$ Deg., $\phi_s = 0$ Deg.

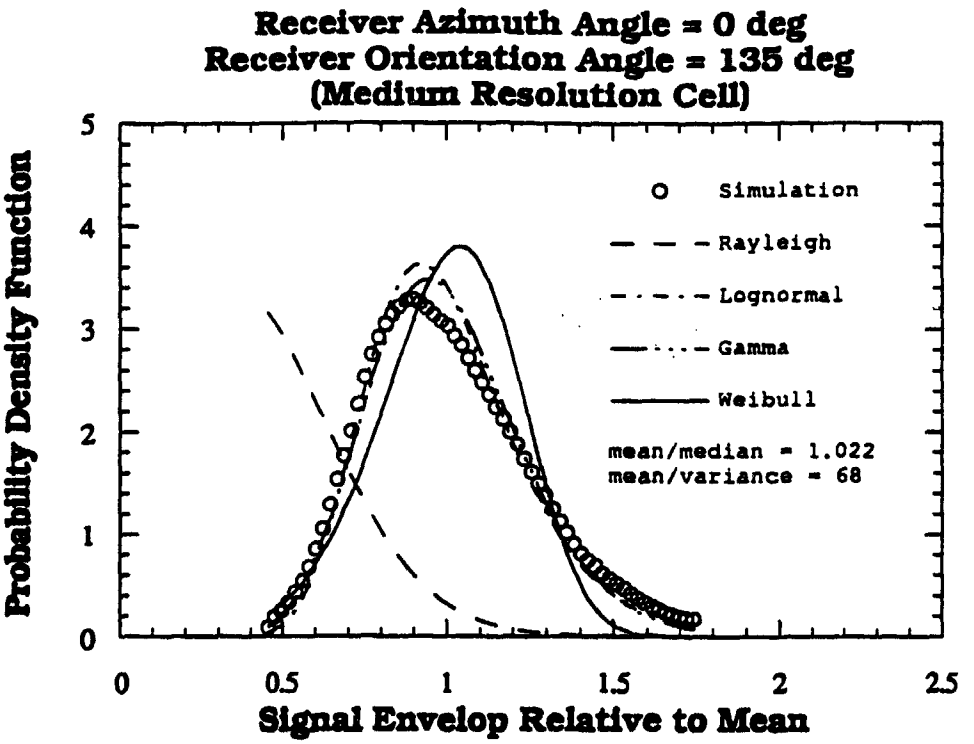

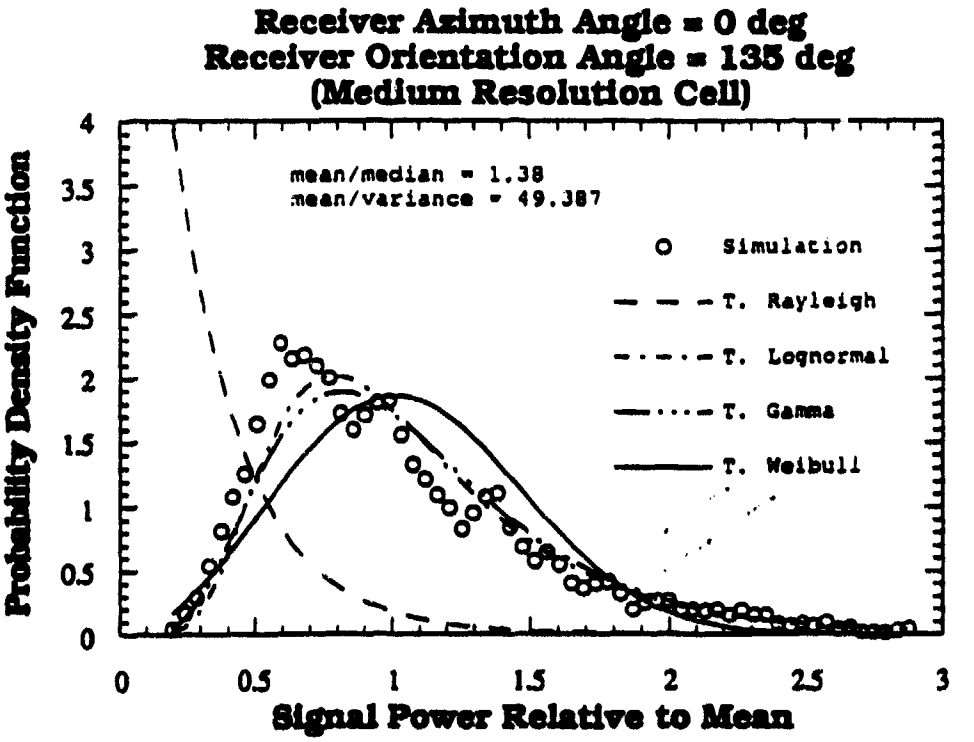

Figure B5b. Comparison between statistical models and simulated data for the medium cell size.

Table 5b

Signal Envelope

Model	RMS Error	Model Parameters	
		shape	scale
Rayleigh	2.941		0.10
Lognormal	0.231	-1.35	0.24
Gamma	0.198	17.3	0.015
Weibull	0.945	5.34	0.29
mean= 2.7e-1		variance= 4.1e-3	

Signal Power

Model	RMS Error	Model Parameters	
		shape	scale
T. Rayleigh	5.214		0.10
T. Lognormal	1.230	-1.35	0.24
T. Gamma	1.213	17.3	0.015
T. Weibull	1.884	5.34	0.29
mean= 7.5e-2		variance= 1.3e-3	

Medium Resolution Cell

Cell Size = 8 Correlation Lengths

$\tau_t = \tau_s = 30$ Deg., $\theta_i = 75$ Deg., $\theta_s = 80$ Deg.,

$\psi_t = 45$ Deg., $\psi_s = 135$ Deg., $\phi_s = 0$ Deg.

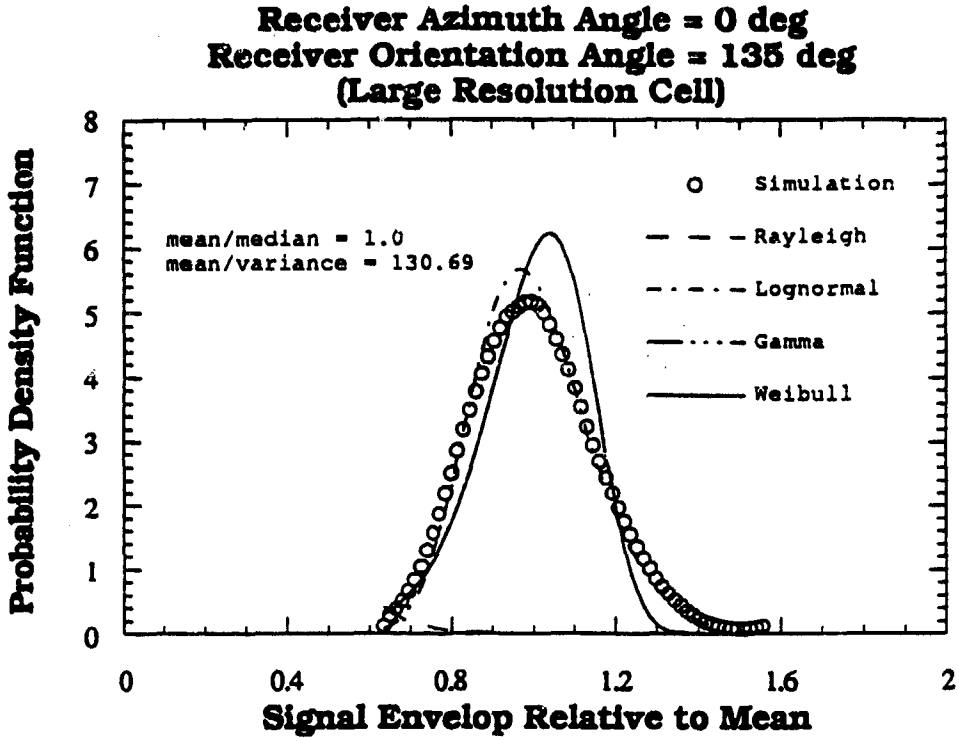

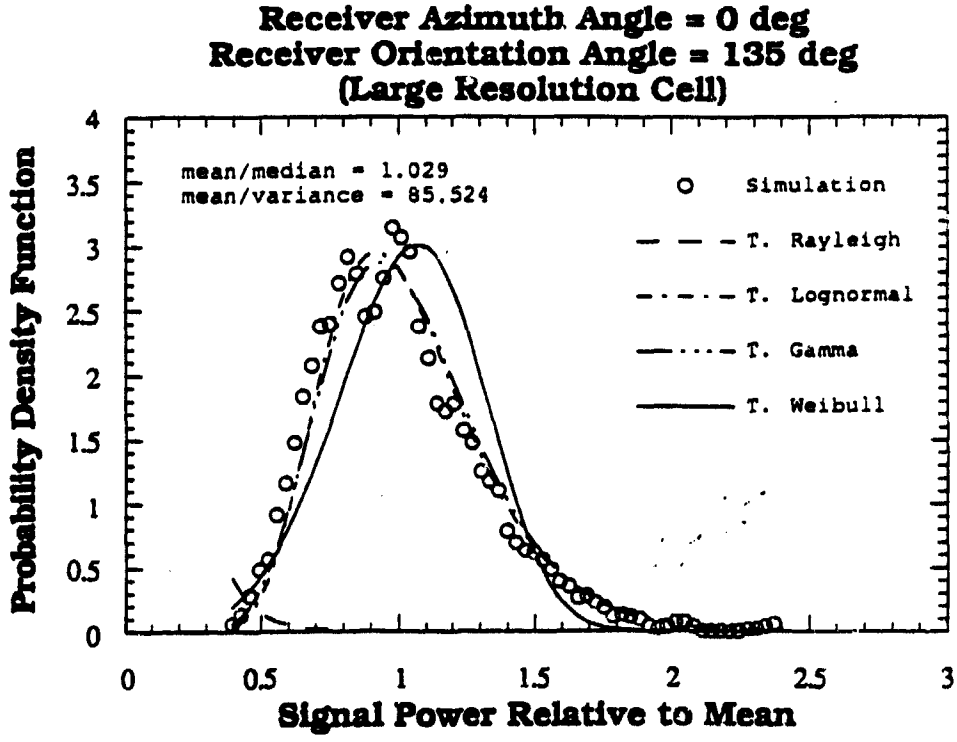

Figure B5c. Comparison between statistical models and simulated data for the large cell size.

Table 5c

Signal Envelope

Model	RMS Error	Model Parameters	
		shape	scale
Rayleigh	2.587		0.083
Lognormal	0.109	-1.01	0.15
Gamma	0.102	45.8	0.008
Weibull	0.561	8.68	0.39
mean= 3.7e-1		variance= 2.9e-3	

Signal Power

Model	RMS Error	Model Parameters	
		shape	scale
T. Rayleigh	3.981		0.083
T. Lognormal	0.757	-1.01	0.15
T. Gamma	0.624	45.8	0.008
T. Weibull	1.207	8.68	0.39
mean= 1.4e-1		variance= 1.6e-3	

Large Resolution Cell

Cell Size = 12 Correlation Lengths

$\tau_t = \tau_s = 30$ Deg., $\theta_i = 75$ Deg., $\theta_s = 80$ Deg.,

$\psi_t = 45$ Deg., $\psi_s = 135$ Deg., $\phi_s = 0$ Deg.

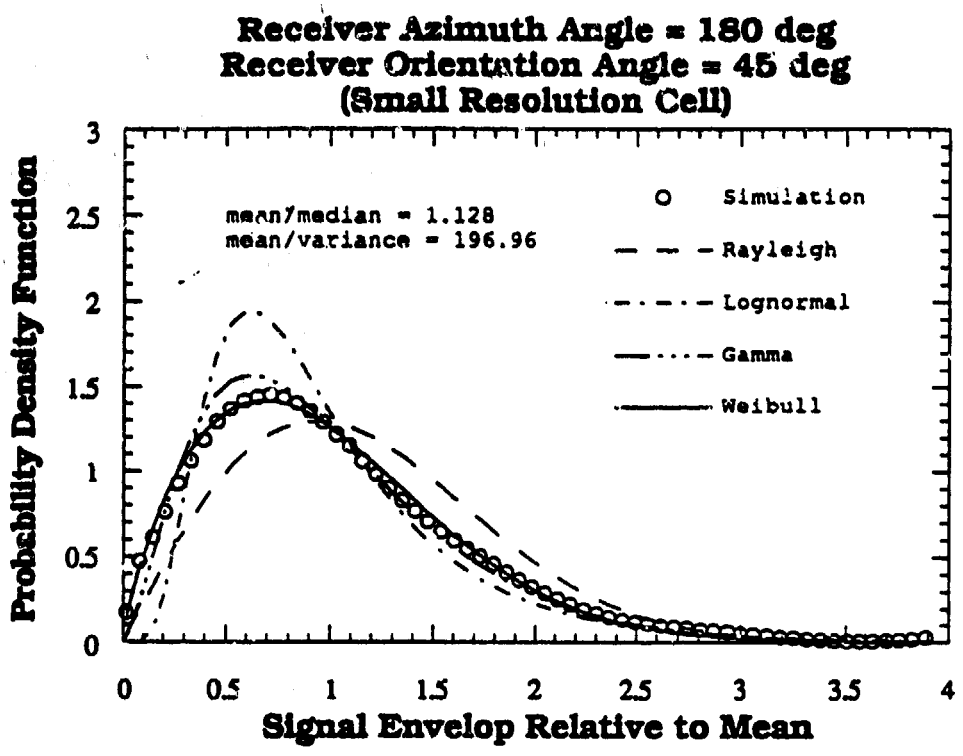

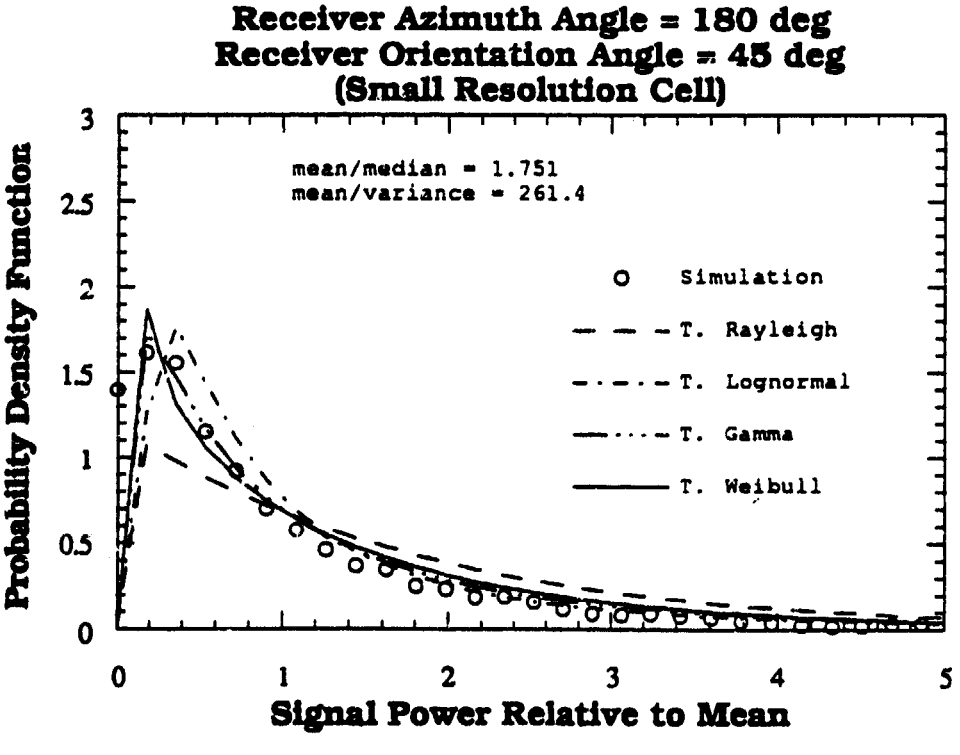

Figure B6a. Comparison between statistical models and simulated data for the small cell size.

Table 6a

Signal Envelope

Model	RMS Error	Model Parameters	
		shape	scale
Rayleigh	5.554		0.013
Lognormal	3.624	-4.45	0.57
Gamma	1.039	2.63	0.005
Weibull	0.874	1.70	0.015
mean= 1.4e-2		variance= 7.0e-5	

Signal Power

Model	RMS Error	Model Parameters	
		shape	scale
T. Rayleigh	120.3		0.013
T. Lognormal	68.25	-4.45	0.57
T. Gamma	40.67	2.63	0.005
T. Weibull	35.62	1.70	0.015
mean= 2.5e-4		variance= 1.0e-7	

Samll Resolution Cell

Cell Size = 4 Correlation Lengths.

$\tau_t = \tau_s = 30$ Deg., $\theta_i = 75$ Deg., $\theta_s = 80$ Deg.,

$\Psi_t = 45$ Deg., $\Psi_s = 45$ Deg., $\phi_s = 180$ Deg.

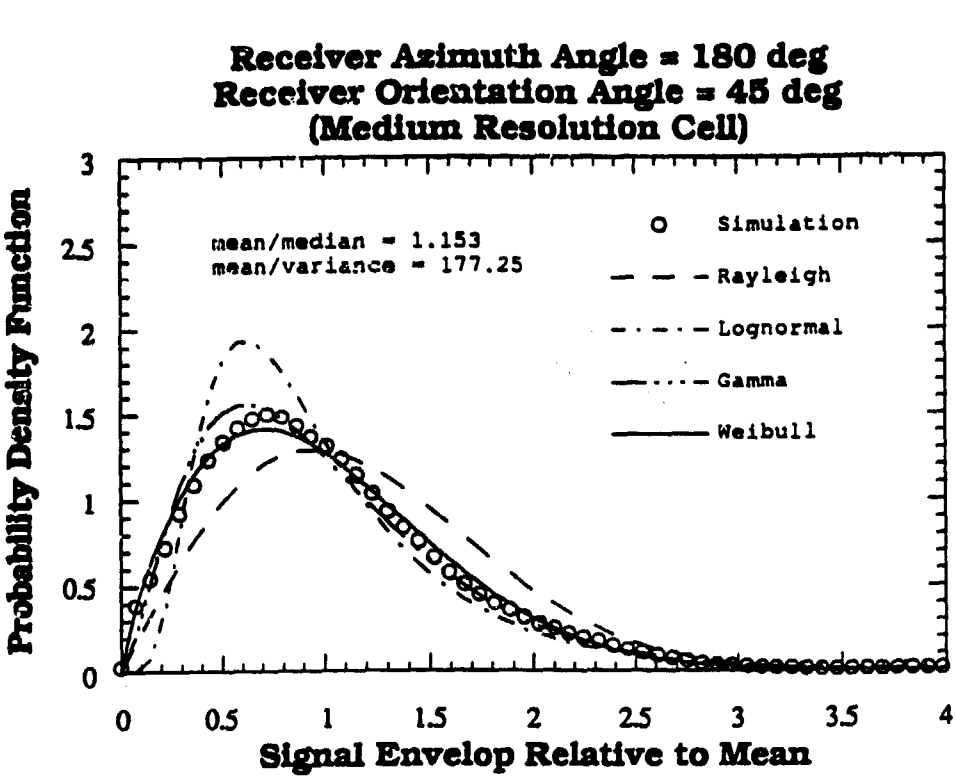

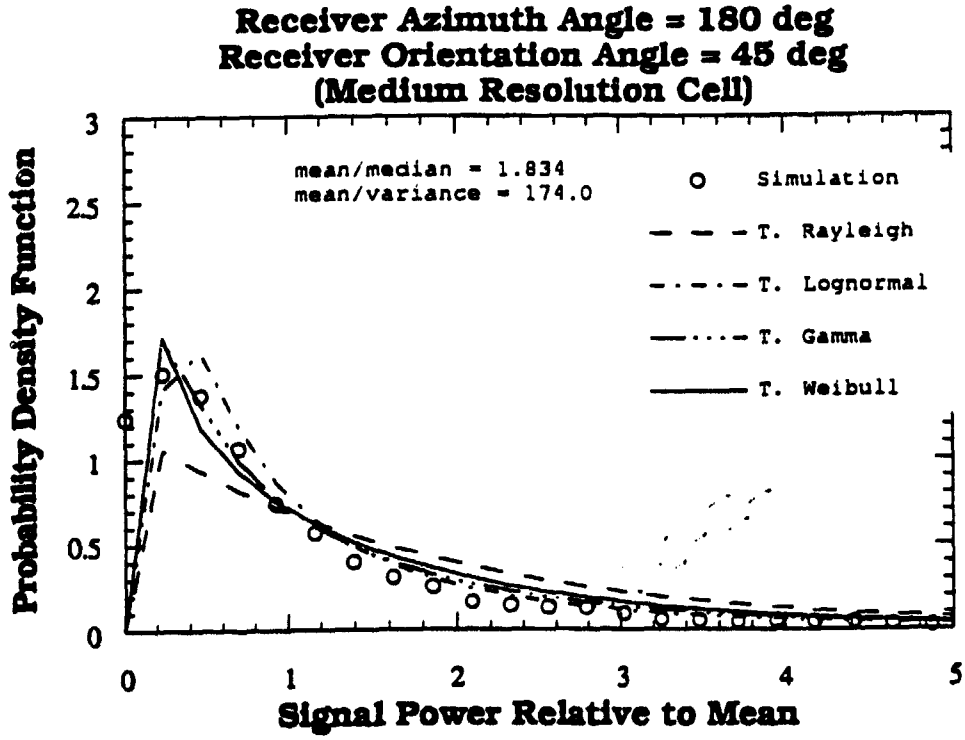

Figure B6b. Comparison between statistical models and simulated data for the medium cell size.

Table 6b

Signal Envelope

Model	RMS Error	Model Parameters	
		shape	scale
Rayleigh	5.331		0.014
Lognormal	2.668	-4.4	0.57
Gamma	1.416	2.59	0.006
Weibull	1.021	1.74	0.017
mean= 1.5e-2		variance= 9.0e-5	

Signal Power

Model	RMS Error	Model Parameters	
		shape	scale
T. Rayleigh	78.25		0.014
T. Lognormal	40.23	-4.4	0.57
T. Gamma	33.57	2.59	0.006
T. Weibull	31.78	1.74	0.017
mean= 3.1e-4		variance= 2.0e-7	

Medium Resolution Cell

Cell Size = 8 Correlation Lengths.

$\tau_t = \tau_s = 30$ Deg., $\theta_i = 75$ Deg., $\theta_s = 80$ Deg.,

$\Psi_t = 45$ Deg., $\Psi_s = 45$ Deg., $\phi_s = 180$ Deg.

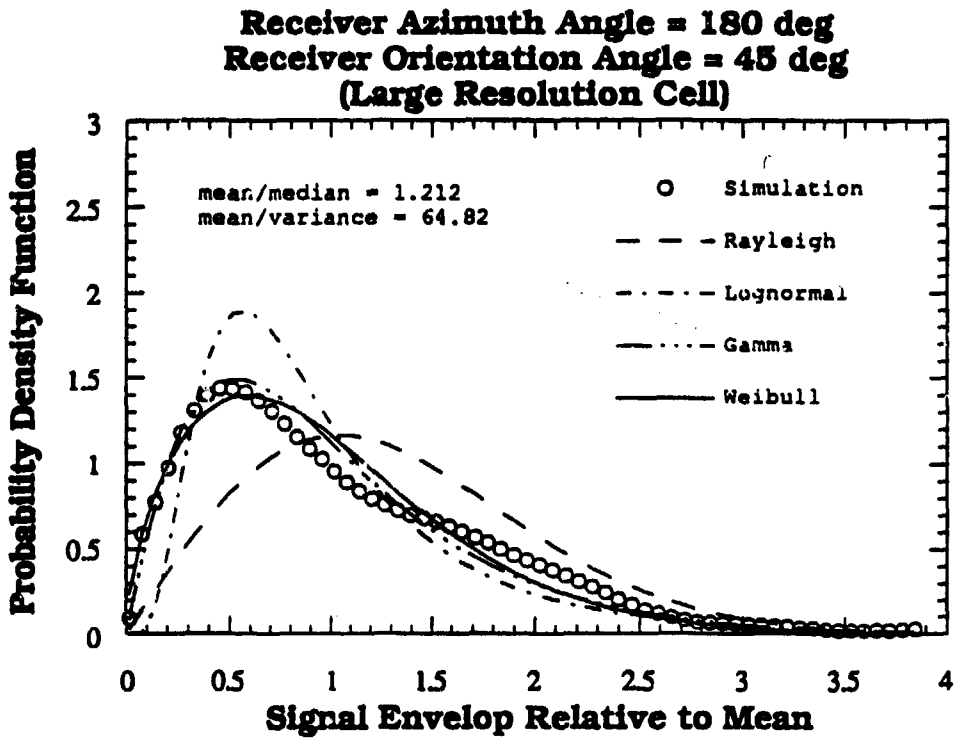

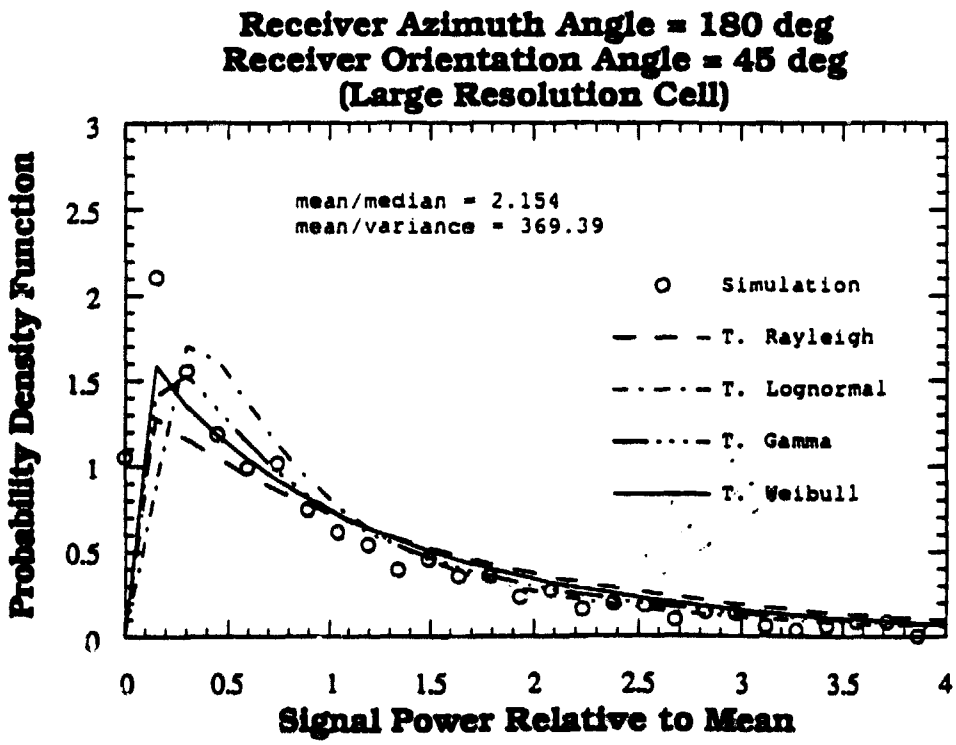

Figure B6c. Comparison between statistical models and simulated data for the large cell size.

Table 6c

Signal Envelope

Model	RMS Error	Model Parameters	
		shape	scale
Rayleigh	3.658		0.035
Lognormal	2.947	-3.57	0.61
Gamma	1.087	2.20	0.015
Weibull	1.023	1.59	0.037
mean= 3.4e-2		variance= 5.0e-4	

Signal Power

Model	RMS Error	Model Parameters	
		shape	scale
T. Rayleigh	27.54		0.035
T. Lognormal	19.27	-3.57	0.61
T. Gamma	12.03	2.20	0.015
T. Weibull	12.92	1.59	0.037
mean= 1.6e-3		variance= 4.4e-6	

Large Resolution Cell

Cell Size = 12 Correlation Lengths

$\tau_t = \tau_s = 30$ Deg., $\theta_i = 75$ Deg., $\theta_s = 80$ Deg.,

$\Psi_t = 45$ Deg., $\Psi_s = 45$ Deg., $\phi_s = 180$ Deg.

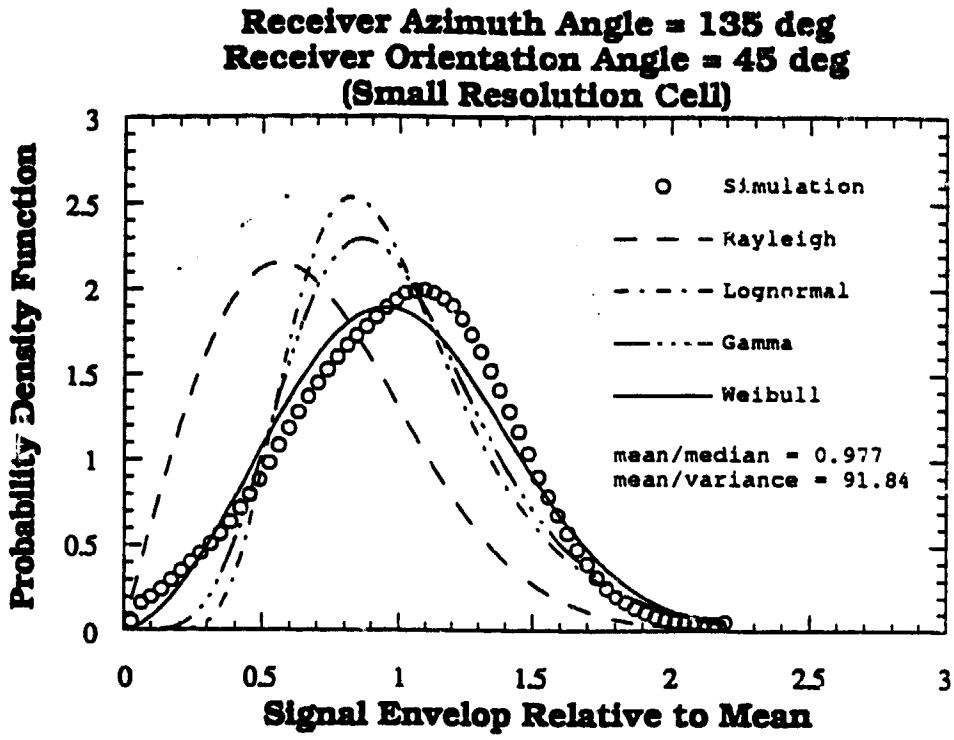

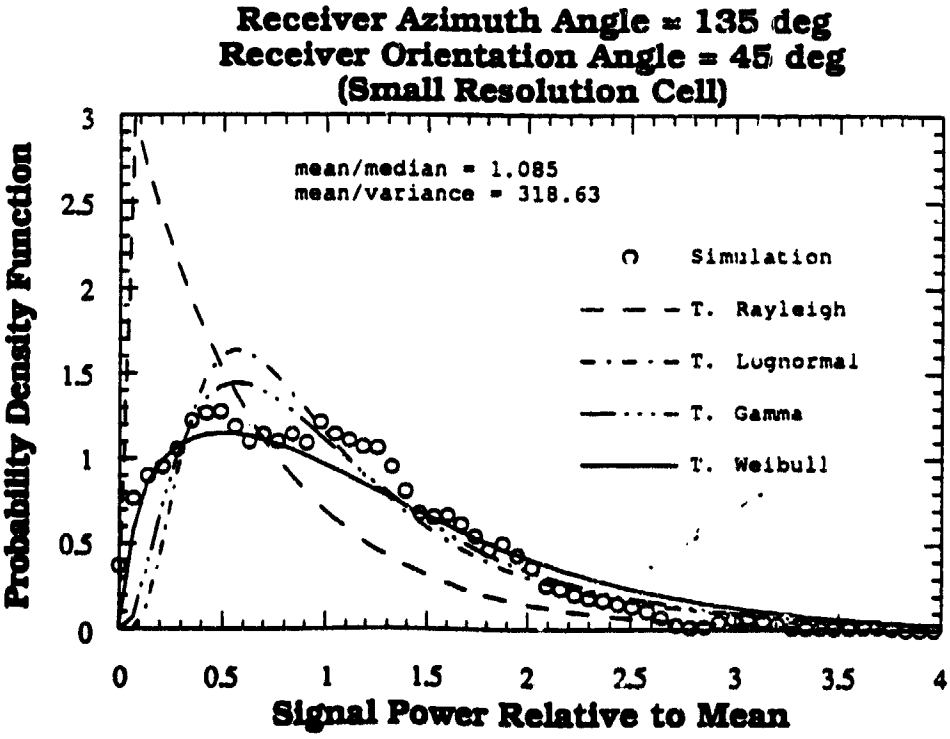

Figure B7a. Comparison between statistical models and simulated data for the small cell size.

Table 7a

Signal Envelope

Model	RMS Error	Model Parameters	
		shape	scale
Rayleigh	3.921		0.046
Lognormal	1.926	-2.591	0.36
Gamma	1.914	7.05	0.011
Weibull	1.288	2.57	0.091
mean= 8.0e-2		variance= 9.0e-4	

Signal Power

Model	RMS Error	Model Parameters	
		shape	scale
T. Rayleigh	21.22		0.046
T. Lognormal	13.29	-2.591	0.36
T. Gamma	13.56	7.05	0.011
T. Weibull	10.94	2.57	0.091
mean= 7.3e-3		variance= 2.3e-5	

Small Resolution Cell

Cell Size = 4 Correlation Lengths

$\tau_t = \tau_s = 30$ Deg., $\theta_i = 75$ Deg., $\theta_s = 80$ Deg.,

$\Psi_t = 45$ Deg., $\Psi_s = 45$ Deg., $\phi_s = 135$ Deg.

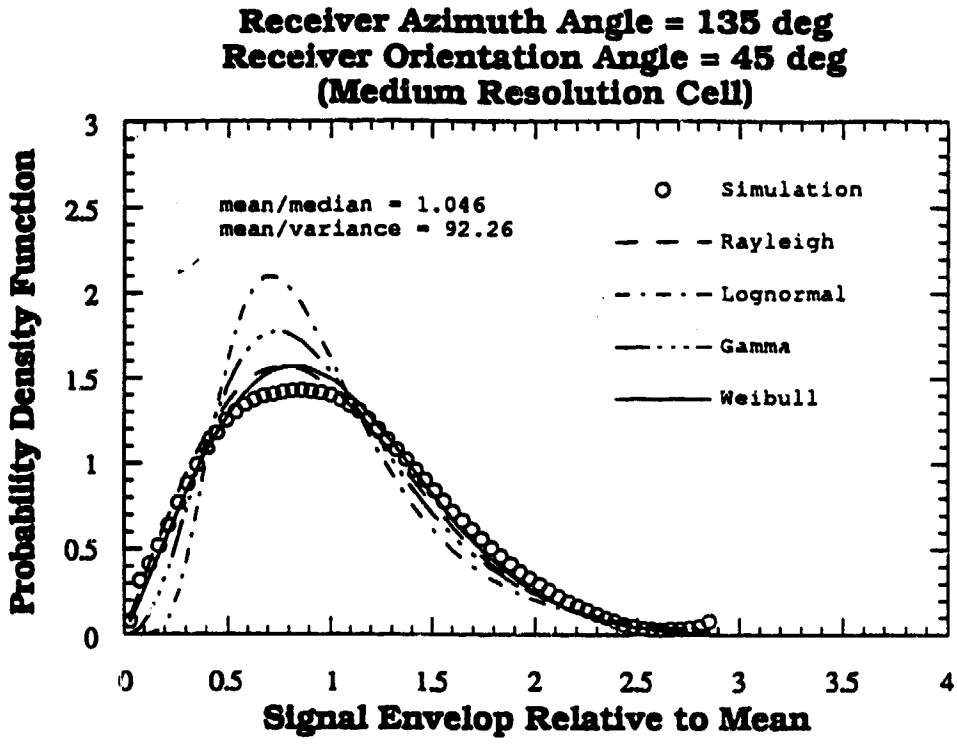

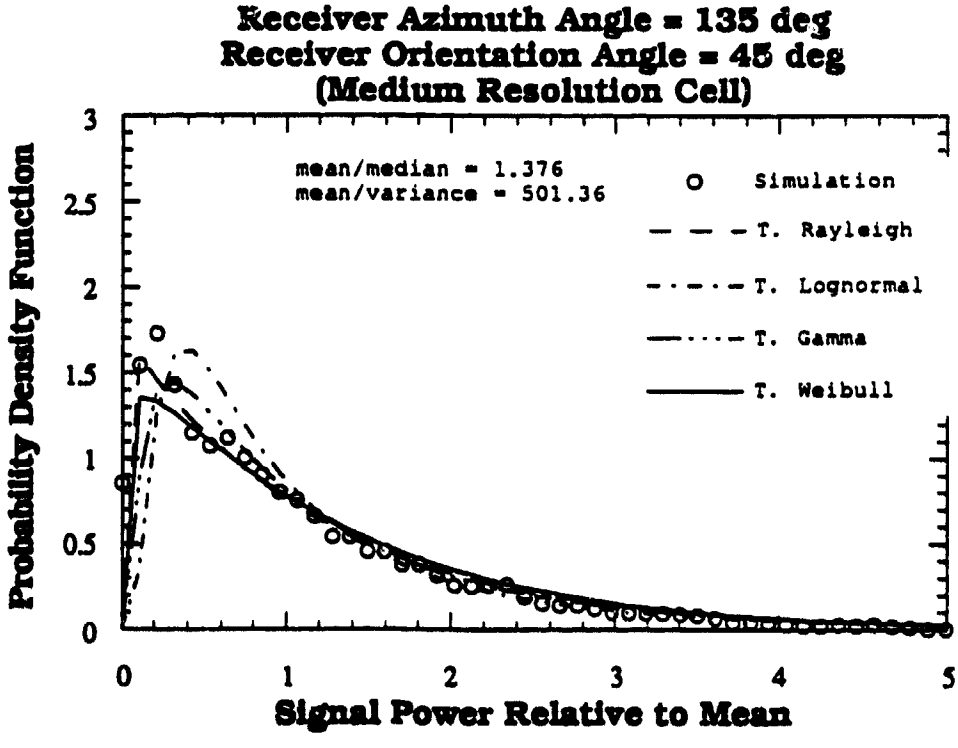

Figure B7b. Comparison between statistical models and simulated data for the medium cell size.

Table 7b

Signal Envelope

Model	RMS Error	Model Parameters	
		shape	scale
Rayleigh	0.647		0.033
Lognormal	2.666	-3.28	0.48
Gamma	1.651	3.79	0.011
Weibull	0.524	2.03	0.048
mean= 4.3e-2		variance= 5.0e-4	

Signal Power

Model	RMS Error	Model Parameters	
		shape	scale
T. Rayleigh	13.03		0.033
T. Lognormal	22.48	-3.28	0.48
T. Gamma	15.31	3.79	0.011
T. Weibull	12.88	2.03	0.048
mean=2.2e-3		variance= 4.0e-6	

Medium Resolution Cell

Cell Size = 8 Correlation Lengths

$\tau_t = \tau_s = 30$ Deg., $\theta_i = 75$ Deg., $\theta_s = 80$ Deg.,

$\Psi_t = 45$ Deg., $\Psi_s = 45$ Deg., $\phi_s = 135$ Deg.

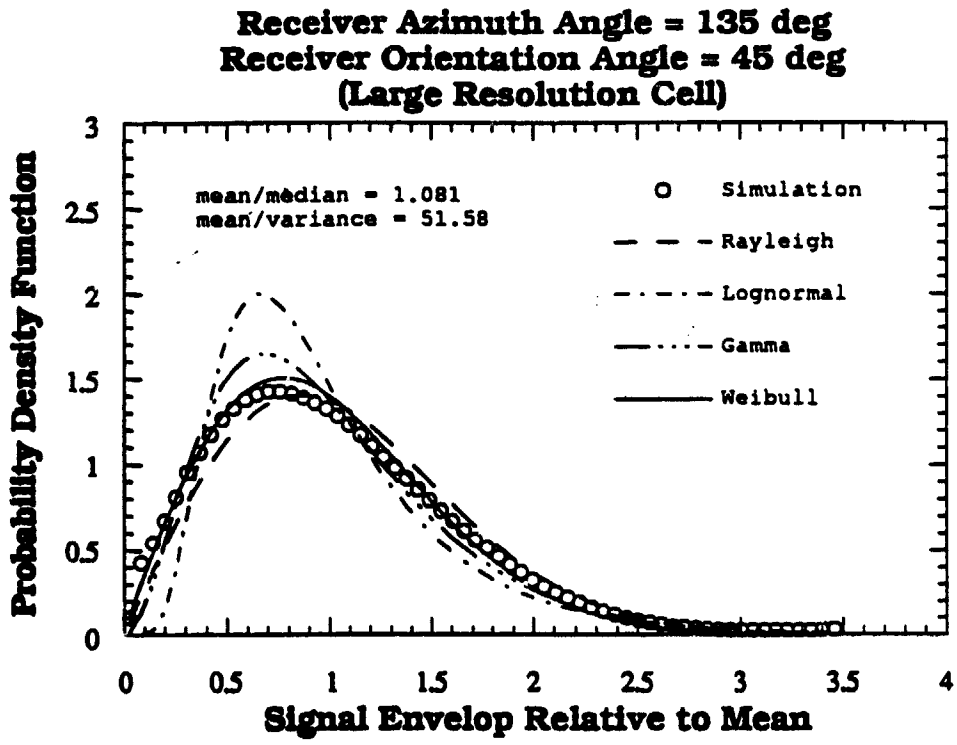

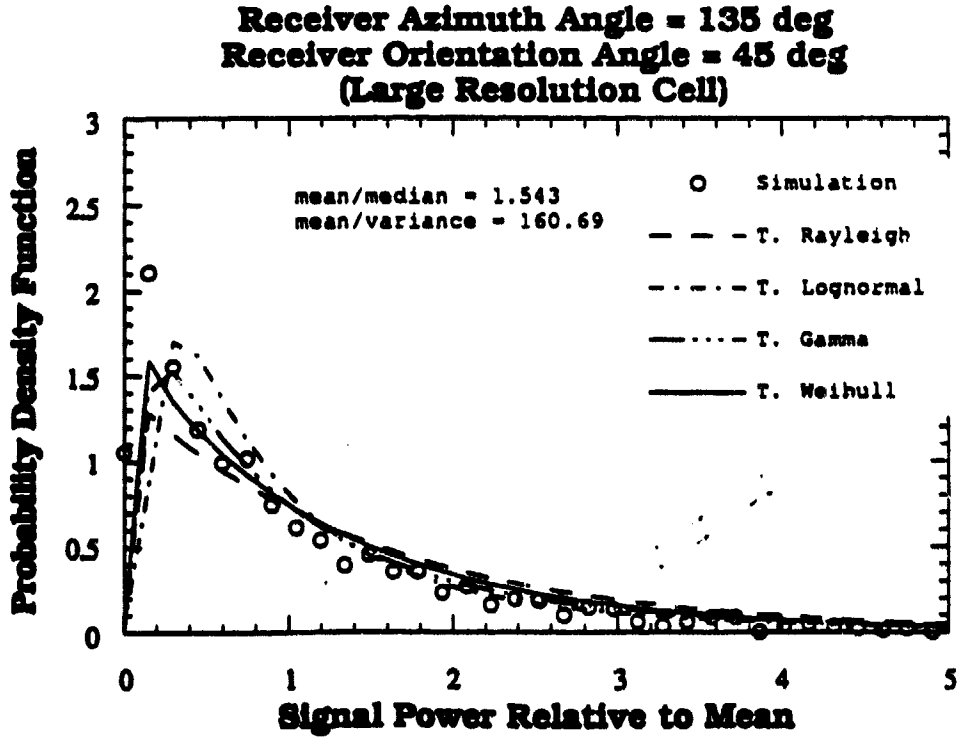

Figure B7c. Comparison between statistical models and simulated data for the large cell size.

Table 7c

Signal Envelope

Model	RMS Error	Model Parameters	
		shape	scale
Rayleigh	0.728		0.05
Lognormal	0.736	-2.9	0.50
Gamma	0.726	3.10	0.02
Weibull	0.430	1.90	0.069
mean= 6.1e-2		variance=1.2e-3	

Signal Power

Model	RMS Error	Model Parameters	
		shape	scale
T. Rayleigh	5.338		0.05
T. Lognormal	5.989	-2.9	0.50
T. Gamma	4.213	3.10	0.02
T. Weibull	4.581	1.90	0.069
mean=5.0e-3		variance= 3.0e-5	

Large Resolution Cell

Cell Size = 12 Correlation Lengths

$\tau_t = \tau_s = 30$ Deg., $\theta_i = 75$ Deg., $\theta_s = 80$ Deg.,

$\psi_t = 45$ Deg., $\psi_s = 45$ Deg., $\phi_s = 135$ Deg.

*U.S. GOVERNMENT PRINTING OFFICE: 1994-510-117-50057